



Review

Mineralogy and genetic features of the Cu-As-Ni-Sb-Pb mineralization from the Mlakva polymetallic deposit (Serbia) – New occurrence of (Ni-Sb)-bearing Cu-arsenides



Ana S. Radosavljević-Mihajlović^a, Jovica N. Stojanović^{a,*}, Slobodan A. Radosavljević^a, Aleksandar M. Pačevski^b, Nikola S. Vuković^c, Radule D. Tošović^d

^a Applied Mineralogy Unit, Institute for Technology of Nuclear and Other Mineral Raw Materials, Franchet d'Esperey 86, P.O. Box 390, 11000 Belgrade, Serbia

^b Department of Mineralogy and Petrology, Faculty of Mining and Geology, University of Belgrade, Djušina 7, 11000 Belgrade, Serbia

^c Laboratory for Scanning Electron Microscopy, Faculty of Mining and Geology, University of Belgrade, Djušina 7, 11000 Belgrade, Serbia

^d Department of Economic Geology, Faculty of Mining and Geology, University of Belgrade, Djušina 7, 11000 Belgrade, Serbia

ARTICLE INFO

Article history:

Received 2 February 2016

Received in revised form 23 August 2016

Accepted 26 August 2016

Available online 22 September 2016

Keywords:

β -domeykite

Ni-bearing koutekite

(Ni-Sb)-bearing α -domeykite

Arsenical breithauptite

Nickeline

Boranja ore field

ABSTRACT

(Ni-Sb)-bearing Cu-arsenides are rare minerals within the Mlakva and Kram mining sectors (Boranja ore field) one of the less-known Serbian Cu deposits. (Ni-Sb)-bearing Cu-arsenides were collected from the Mlakva skarn-replacement Cu(Ag,Bi)-FeS polymetallic deposit. The identified phases include β -domeykite, Ni-bearing koutekite and (Ni-Sb)-bearing α -domeykite. (Ni-Sb)-bearing Cu-arsenides are associated with nickeline, arsenical breithauptite, chalcocite, native Ag, native Pb and litharge. Pyrrhotite, pyrite, chalcopyrite, cubanite, bismuthinite, molybdenite, sphalerite, galena, Pb(Cu)-Bi sulfosalts and native Bi, as well as minor magnetite, scheelite and powellite are associated with the sulfide paragenesis. The electron microprobe analyses of the (Ni-Sb)-bearing Cu-arsenides yielded the following average formulae: $(\text{Cu}_{2.73}\text{Ni}_{0.17}\text{Fe}_{0.03}\text{Ag}_{0.01})_{\Sigma 2.94}(\text{As}_{0.98}\text{Sb}_{0.05}\text{S}_{0.02})_{\Sigma 1.06}$ - β -domeykite (simplified formula $(\text{Cu}_{2.7}\text{Ni}_{0.2})_{\Sigma 2.9}\text{As}_{1.1}$); $(\text{Cu}_{3.40}\text{Ni}_{1.40}\text{Fe}_{0.11})_{\Sigma 4.91}(\text{As}_{1.94}\text{Sb}_{0.13}\text{S}_{0.02})_{\Sigma 2.08}$ -Ni-bearing koutekite (simplified formula $(\text{Cu}_{3.4}\text{Ni}_{1.5})_{\Sigma 4.9}\text{As}_{2.1}$); and $\text{Cu}_{1.97}(\text{Ni}_{0.98}\text{Fe}_{0.03})_{\Sigma 1.01}(\text{As}_{0.81}\text{Sb}_{0.22})_{\Sigma 1.03}$ -Ni-bearing α -domeykite (simplified formula Cu_2NiAs). The Rietveld refinement yielded the following unit-cell parameters for β -domeykite and Ni-bearing koutekite: $a = 7.1331(4)$; $c = 7.3042(5)$ Å; $V = 321.86(2)$ Å³, and $a = 5.922(4)$; $b = 11.447(9)$; $c = 5.480(4)$ Å; $V = 371.48(5)$ Å³, respectively. Ore geology, paragenetic assemblages and genesis of the Mlakva deposit are discussed in detail and the Cu-As-Ni-Sb-Pb mineralization has been compared with similar well-known global deposits.

© 2016 Elsevier B.V. All rights reserved.

Contents

1. Introduction	1246
2. Geological setting and metallogeny of the Boranja ore field	1246
2.1. Geological settings and description of the Mlakva and Kram mining sectors	1246
3. Materials and methodology	1248
4. Bulk ore geochemistry	1250
5. Ore mineralogy	1251
5.1. Pyrrhotite-chalcopyrite-pyrite and Pb(\pm Cu)-Bi sulfosalts mineral assemblage	1251
5.2. (Ni-Sb)-bearing Cu-arsenides mineral assemblage with native Ag and Pb	1252
5.3. Genetic features of the Mlakva Cu deposit and the Cu-As-Ni-Sb-Pb mineralization	1253
6. Crystallographic investigations	1255
7. Discussion and conclusions	1256
Acknowledgments	1257
References	1257

* Corresponding author.

1. Introduction

The Cu-Ni-bearing arsenides and alloy-like compounds generally belong to the sulfides, arsenic sub-class, because As has very similar crystallochemical properties to S (Dana, 2008). Until now, there are > 10 defined natural Cu- and Ni-arsenides (algononite Cu_6As , α - and β -domeykite Cu_3As , koutekite $\text{Cu}_2\text{As}-\text{Cu}_5\text{As}_2$, etc.) and (maucherite $\text{Ni}_{11}\text{As}_8$, nickeline NiAs , rammelsbergite NiAs_2 , etc.) (Ramdohr, 1980). Breithauptite is a Ni-antimonide mineral with the simple formula NiSb . It occurs in hydrothermal calcite veins associated with Co-Ni-Ag ores (Anthony et al., 1990).

Copper and Ni, adjacent elements in the Periodic Table of Elements, when alloyed form a complete solid solution series. One can expect that the mechanical properties of the ternary alloy with As will prove similar to those of Cu-As alloys (As bronze), which, when compared with Cu-Sn alloys (Sn bronze), exhibit high hardness combined with high ductility (Lechtman, 1996). In nature, only minerals from the Cu-As and Ni-As binary system are determined, while minerals from the Cu-Ni binary system do not exist (Subramanian and Launghlin, 1988). The Cu-Ni binary system is a simple isomorphous system with indications of clustering of atoms at ~50 at.% Ni and $T < 350^\circ\text{C}$ (Gupta, 2000). Depending upon the relative amounts of As and Ni present, the color can range from pale yellow to bright yellow (Uhland et al., 2001).

Cu-Ni-bearing arsenides are deposited as fine and complex spherical and/or kidney-like aggregates, composed of two or more intimately intergrown individuals of various dimensions (mm- μm -nm). This greatly complicates their determination, even by an Electron Microprobe. In addition, the closeness of the chemical composition of these minerals contributes to their similar optical and other physical properties, which makes even more difficult their individual identification (Ramdohr, 1980). According to the reflectance spectra, these alloy-like minerals are between galena (R~42%) and pyrite (R~53%) (Makovicky and Johan, 1978).

Occurrences and mineral systems of Cu-Ni bearing arsenides worldwide are few and include: Černý Důl, Krkonoše, Bohemia, Czech Republic (Johan, 1958, 1960, 1961, 1985), the Mohawk No 2 mine, Mobawk, Keweenaw Co., Michigan, USA (Moore, 1971), the Anarak District, central Iran (Tarkian et al., 1983), Cu-mineralized sandstone in Kazakhstan (Abulgazina et al., 1991).

Copper-arsenides and arsenates are not rare in sulfide deposits, and have been discovered in the following locations: Chile, Bolivia, Mexico, USA, Canada, Sweden, Austria, Czech Republic, France, Germany, Great Britain, Iran, and several other occurrences (Pierrot et al., 1974; Iglesias and Nowacki, 1977; Picot and Ruhlmann, 1978; Paar and Meixner, 1979; Anthony et al., 1990; Sarp and Černý, 2001; Černý et al., 2003). They are commonly placed in supergene zones of primary Cu-sulfide deposits. Domeykite, the most abundant Cu-arsenide, was first discovered in Cu mines in Chile. Domeykite has two polymorphic modifications: cubic α -domeykite is stable at temperatures $< 225^\circ\text{C}$; hexagonal β -domeykite is stable in the range from 225 to 827°C . In nature, β -domeykite occurs usually in high-temperature hydrothermal deposits in association with kutinaite, löllingite, and dyscrasite (Chvilyova et al., 1988). The phase $\text{Cu}_{5-x}\text{As}_2$ has two modifications. The high-temperature cubic form decomposes peritectically to β -domeykite and native arsenic between 340 and 360°C . If quenched, the high-temperature phase transforms at 315°C into a low-temperature, orthorhombic modification identical to koutekite (Juzá and von Benda, 1968; Liebisch and Schubert, 1971; Picot and Vernet, 1967). Other Cu-arsenides with Ag and Au are very rare, and occur in low-temperature hydrothermal deposits as products of supergene alterations of Cu-sulfides (Hak et al., 1970).

Native metals and their alloys (Au, Ag, Bi, As, AuTe, AuAg, NiSb, and AsSb) are common in the polymetallic deposits of the Boranja ore field (Radosavljević, 1988; Radosavljević-Mihajlović et al., 2007; Radosavljević et al., 2014). The present study focuses on the new minerals of (Ni-Sb)-bearing Cu-arsenides within the skarn-replacement

hydrothermal ores from the Mlakva Cu(Ag,Bi)-FeS polymetallic deposit. A special review is given on their paragenetic relationships, and the genetic significance of mineral associations as indicators of ore formation conditions. Mineralogical, chemical and crystallographic data of β -domeykite, Ni-bearing koutekite, (Ni-Sb)-bearing α -domeykite, arsenical breithauptite, and nickeline are also discussed in detail.

2. Geological setting and metallogeny of the Boranja ore field

The Podrinje metallogenic district (PMD) belongs to the Serbo-Macedonian Metallogenic Province (SMMP) and includes several smaller ore fields: Boranja (Serbia), Cer (Serbia), and Srebrenica (Bosnia and Herzegovina) (Janković, 1990). The Boranja ore field (BOF) covers an area of about 200 km². It consists of Paleozoic, Mesozoic, and Tertiary rocks (Fig. 1). The Paleozoic is represented by Carboniferous sediments, mostly slates and sandstones of low-grade metamorphism, as well as by limestones (the "Drina Series"). The Mesozoic complex consists of Triassic, Jurassic and Cretaceous rocks, mostly slates, limestones, volcanic sediments, mafic and ultramafic rocks. The Mlakva deposit, situated on the SE margin of the Boranja Oligocene granodiorite intrusive (Karamata, 1955; Delaloye et al., 1989; Steiger et al., 1989), belongs to the Dinaridic granitoid suite of Late Paleogene – Early Neogene age (Cvetković et al., 2000, 2004), and is situated on the border of three terranes – the Jadar block terrane, the Vardar zone composite terrane and the Drina – Ivanjica terrane (Karamata and Krstić, 1996; Karamata et al., 1990).

The BOF consists of a large number of sulfide deposits with Pb, Zn, Sb, Cu, Bi and Mo. Small magnetite deposits are connected to the skarn (pyrometasomatic) stage (Fig. 1). Skarns of Ca-type were formed along contacts of the Triassic limestones and the Boranja granodiorite intrusive. The most important deposits of the BOF are: Brasina-Zajača-Stolice Sb-ore zone; Veliki Majdan Pb(Ag)-Zn-FeS₂, Ravnaja Pb-Zn-CaF₂ and Rujevac Sb-Pb-Zn-As. Minerals of the BOF were deposited in several successive stages, corresponding to a single regional-scale mineralization event genetically related to the subvolcanic-plutonic intrusions of the Boranja magmatic complex. This can be best demonstrated by the zonal arrangement of several mineral associations [Fe-Cu(Bi) → Pb(Ag)-Zn → Sb(As,Pb-Zn) → CaF₂(Pb-Zn)], with increasing distance from the Boranja granodiorite (Radosavljević et al., 2013).

The Mlakva deposit is situated on the southern slopes of Jagodnja Mountain, 115 km to the SW from Belgrade, in the village of Crnča located 9 km SSW from Krupanj (Fig. 1). The Cu mineralization, hosted in the contact-metamorphic zone of Boranja granodiorite, was formed by the intrusion of granodiorite magma into the sediments of the Diabase-Chert Formation (DCF). Within this mineralization, two close ore-bearing areas, the Mlakva and Kram mining sectors, have been recognized. The shortest distance between these ore-bearing areas (WSW-ENE direction) is approximately 500 m (Fig. 1). The younger hydrothermal mineralization was deposited during multiphase volcanism in the pre-existing contact metamorphic zone. These events had influence on forming polymetallic Cu orebodies of different shapes and sizes.

2.1. Geological settings and description of the Mlakva and Kram mining sectors

The oldest lithostratigraphic unit, which characterizes the Mlakva and Kram mining sectors, consists of the DCF kinds, which belong to the Middle and Upper Jurassic. The DCF by itself is a complex lithological terrain typical for ophiolitic mélange. It is composed of different sedimentary and metamorphic lithologies (limestones, marlstone, alevrolytes, metapelite, sandstones, metasandstones, marble, marbled limestone, quartz sericite schist, chlorite sericite schist, chlorite amphibole schists and albite-chlorite schist) and products of basic and ultrabasic magmatism – diabase, spilite, gabbro, gabbro diabase, gabbro diorite, peridotite, serpentised peridotite, serpentinite and dunite (Fig. 2a).

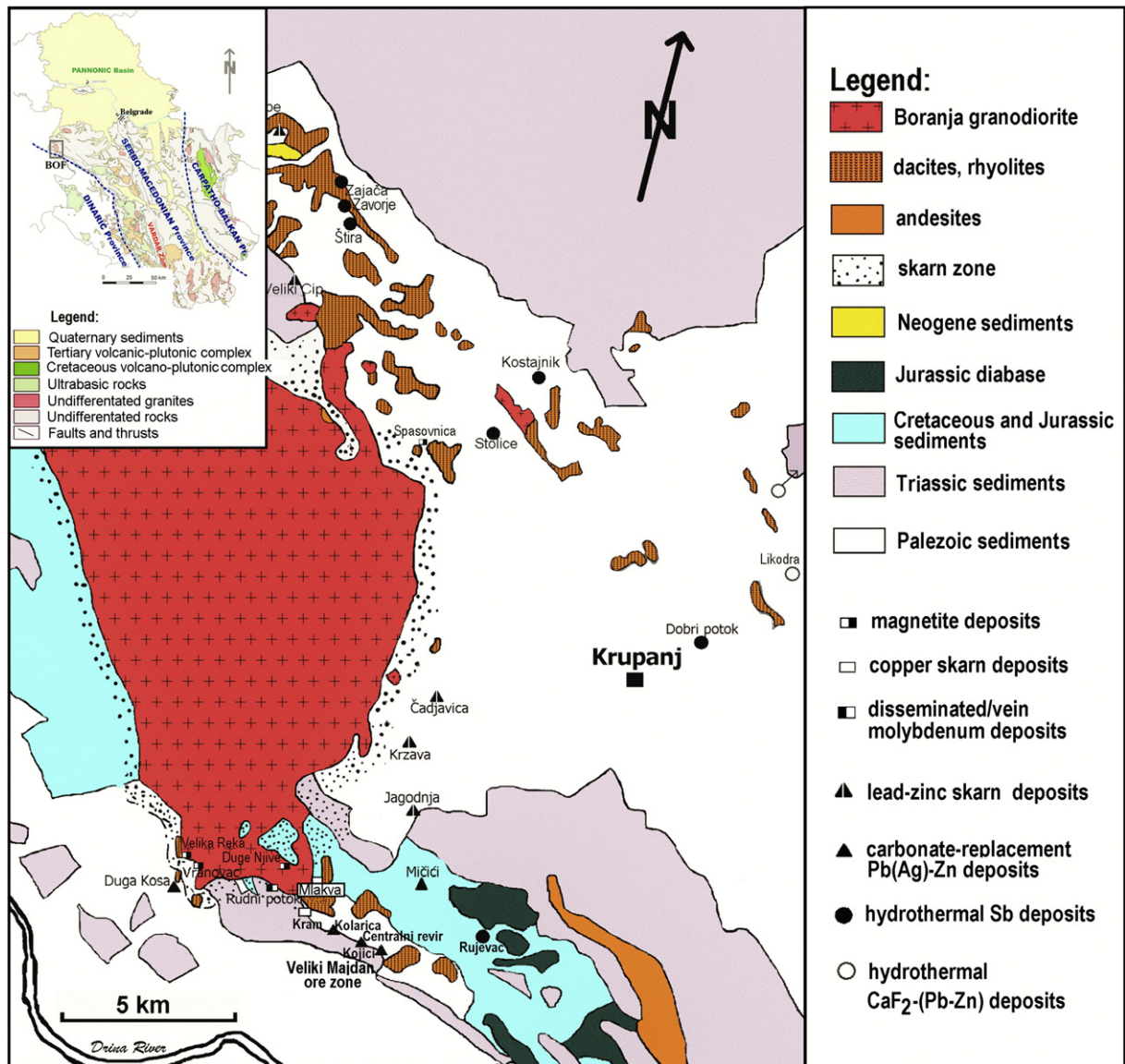


Fig. 1. Detailed geological and metallogenic map of the BOF and a position of the Mlakva deposit (modified according to Basic Geological Map of Serbia, 1:100,000). Upper left corner shows exact location of BOF within Serbia (Monthel et al., 2002).

Development of the Boranja granodiorite massif is related to multi-stage magmatic activity, which has caused the formation of a large number of granitoid rocks such as syenite over quartz syenite, quartz monzonite, quartz diorite, granodiorite and other equivalents of granitoid-magma, whereas in the early stages of igneous activity, lamprophyres were emplaced (Prelević et al., 2004).

During Oligocene time granitoid magma intruded the Boranja granodiorite massif. Volcanic activity caused the formation of dikes and rare effusion of dacite and andesite into their transitional varieties of volcanics. Eruption of pyroclastic rocks completed the volcanic cycle in this area.

In the area of the Mlakva and Kram mining sectors, a large number of different contact-metamorphic rocks were formed (dependant on the protolith types and distance from the magmatic intrusions). Skarn protoliths are olistolithic limestones from the DCF and are more prevalent at the Kram location. They occur in several varieties with the most common being epidosite, pyroxenite, and garnetite rocks with accessory magnetite, scheelite and powellite (Radosavljević et al., 2013). Within the non-carbonate rocks, the contact-metamorphic zone contains hornfels, amphibolite, contact-metamorphic diabase, contact-metamorphic peridotite and other contact-metamorphic rocks. These

rocks are grouped under the general name contact-rocks as shown in Fig. 2a–c.

In the Mlakva tabular copper deposit, mineral deposition is primarily by metasomatic replacement in contact-metamorphic altered peridotites, hornfels and skarns, with subordinate mineralization in felsic-equivalent granitoid-magma, which are mostly represented by dacite and andesite (Fig. 2a). This lenticular swarm is usually formed from several closely lying, parallel, thin tabular ore bodies. The directional extension of the main ore body has been traced for about 250 m, and at depths ranging from a few tens of meters to a maximum of 100 m. The thickness of an integral ore body varies from a few decimeters to a maximum of 16 m as ore zones pinch out along strike at and depth (Fig. 2b–c). The integral orebody has a WSW–ENE trending direction and formed as two subparallel tabular bodies, which join below 150 m in depth (Fig. 2c). The footwall ore body probably pinches out in the contact zone with granodiorite. The hanging wall ore body in the mineralized zone pinches out, significantly reducing its thickness (Pavlović, 2014).

Mineralization is commonly disseminated, but may also be combined with, mm–cm thick veinlets having very different spatial orientations. When the latter occurs, the ore is said to be of the stockwork/

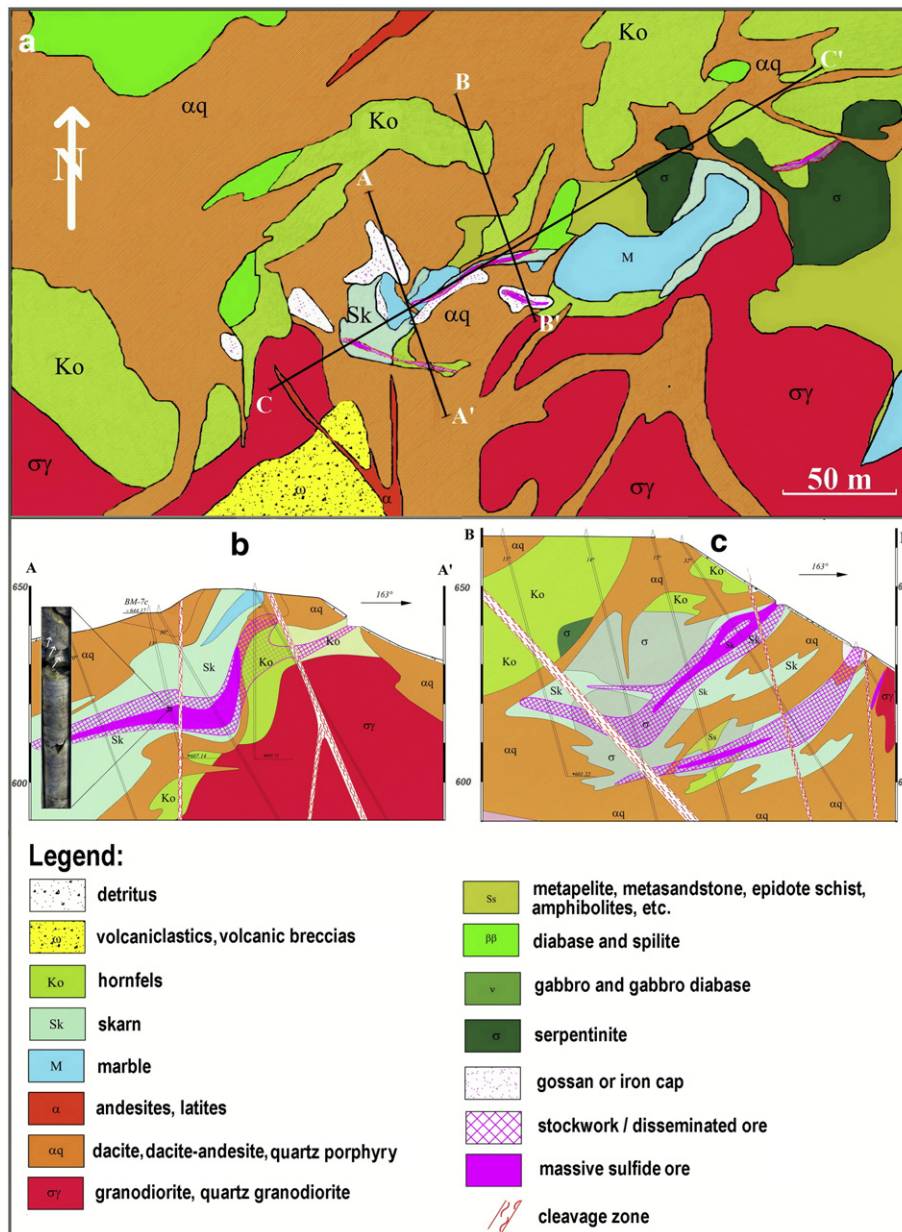


Fig. 2. a) Schematic geological plan of the Mlakva deposit; b) A-A' geological profiles of the Mlakva deposit, with the location of sampling of (Ni-Sb)-bearing Cu-arsenides; and c) B-B' geological profiles of the Mlakva deposit (according to Pavlović, 2014).

disseminated type as shown in Fig. 2b–c. Massive sulfide ore typically occurs in the central parts of both the disseminated and stockwork/disseminated mineralization zones. In the Mlakva copper deposit there are two main ore mineralization types: i) massive sulfide (pyrrhotite-chalcopyrite-pyrite associated with Ag and Bi); and ii) stockwork/disseminated (pyrite-chalcopyrite mineralization). The contact between the massive sulfide and stockwork/disseminated ore is clearly visible, but the boundary between stockwork/disseminated ore and altered skarn is arbitrarily established according to a copper content of >0.3 wt%. The following mineral assemblages were recognized at the Mlakva copper deposit (from early to late): i) garnet-pyroxene with magnetite, scheelite and powellite; ii) pyrrhotite-chalcopyrite-pyrite and Pb(±Cu,Ag)-Bi sulfosalts; iii) (Ni-Sb)-bearing Cu-arsenides with native Ag and Pb; iv) supergene (Table 5).

The most important features of the Kram copper polymetallic deposit were reviewed from Radosavljević-Mihajlović et al. (2007). Collectively, about 2.8 Mt of ore reserves and resources grading 1.02 wt% Cu

and 11.5 g/t Ag have been outlined within the Mlakva and Kram mining sectors by 2014 (Pavlović, 2014).

3. Materials and methodology

Samples were collected from boreholes in the period 2010–2013. (Ni-Sb)-bearing Cu-arsenides were found only in the BM-7c borehole at 25.2 m (Fig. 2, profile AA'). Polished sections were prepared for reflected-light microscopy and Electron Probe Micro-analyses (EPMA), following standard preparation and polishing steps (Picot and Johan, 1982). During the polishing process of (Ni-Sb)-bearing Cu-arsenides kerosene was used in order to prevent oxidation of native lead. The Carl-Zeiss polarizing microscope, model JENAPOL-U equipped with 10×, 20×, 50×, 100× (oil immersion) objectives and a system for a photomicrography (“AxioCam 105 color” camera and “Carl Zeiss AxioVision SE64 Rel. 4.9.1.” software package with „Multiphase” module). The pycnometer method ($V = 5 \text{ ml}^3$) was used for a density measurements

Table 1

Representative average chemical analyses of the Cu-ores and surrounding altered rocks from the BM-7c borehole (Figs. 2b and 3a).

wt%	a.	b.	c.	d.	e.
(n)	(4)	(9)	(5)	(5)	(7)
Cu	<0.01	0.06	0.41	1.19	0.07
Bi	0.009	0.004	0.029	0.072	0.003
Pb	0.004	0.003	0.003	0.004	0.001
Zn	0.010	0.010	0.007	0.016	0.005
Fe	16.01	6.59	21.16	25.83	3.44
As	0.008	0.005	0.007	0.003	0.001
W	0.091	0.054	0.009	0.007	0.003
g/t	a.	b.	c.	d.	e.
Ag	1.2	1.5	3.8	14.4	1.2
Mo	44.5	44.7	18.4	3.2	17.2
Sn	191.9	71.2	53.4	32.0	19.9
Ni	5.1	70.9	51.1	153.2	11.0
Co	5.5	29.8	29.6	70.2	18.5
Sb	0.6	1.9	2.7	2.5	0.9

Note: (n) number of analysis; a) limonitized and altered dacite-andesite; b) altered skarn with a pyrite impregnation; c) stockwork/disseminated Cu-ore; d) massive Cu-ore; e) altered dacite-andesite with a pyrite impregnation.

(in xylene). The reflectance and microhardness measurement were not performed due to very intimate intergrowths of (Ni-Sb)-bearing Cu-arsenides.

EPMA were performed on a JEOL JSM-6610LV scanning electron microscope (SEM) connected with an INCA energy-dispersion X-ray analysis unit; EDX analytical system. An acceleration voltage of 20 kV was used. The samples were not coated with carbon or gold due to its naturally good electrical conductivity. The following standards and analytical lines were used: FeS₂ (FeKα, SKα), Ni (NiKα), Co (CoKα), Cu (CuKα), InAs (As Kα), InSb (SbLα), Ag₂Te (AgLα), PbS (PbMα), and Bi (BiMα). EDX detection limits are 2σ–0.3 wt% (counting time 60 s). General formulae were calculated according to Anthony et al. (1990).

All the elements were determined using ICP-AES and ICP-MS methods (detection limit ~0.05 g/t). X-ray fluorescence spectrometry (XRF) analyses of the samples with (Ni-Sb)-bearing Cu-arsenides (powder) have been carried out by Oxford Instruments, model Lab-× 3500 (detection limit ~0.009 wt%).

The XRD method was used to determine the mineralogical composition, unit-cell parameters of the main minerals and to refine occupancies of mixed Cu/Ni crystallographic sites of β-domeykite and Ni-bearing koutekite by the Rietveld method. The XRD patterns of a powdered sample were obtained using a Philips PW-1710 automated

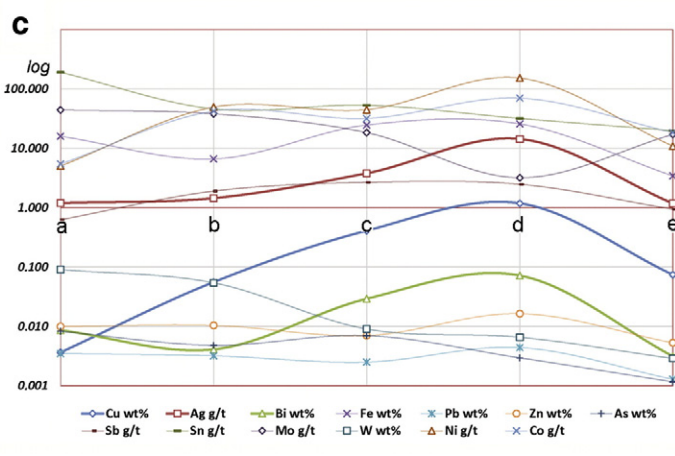
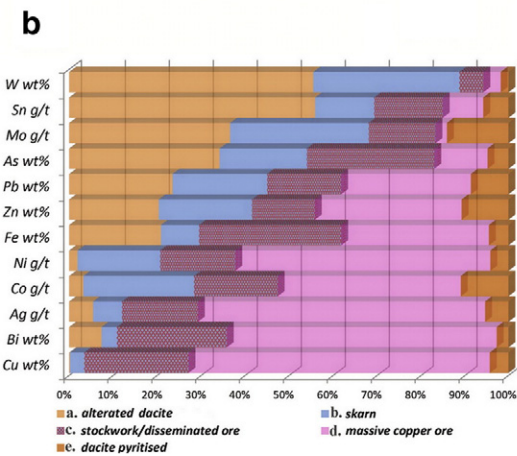
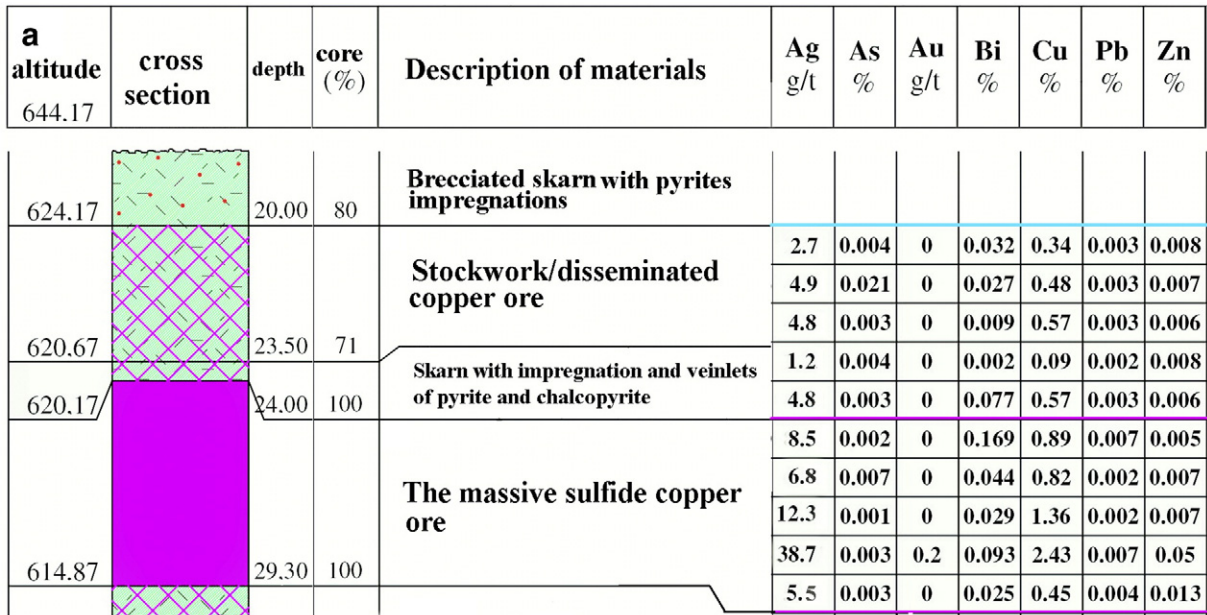


Fig. 3. a) The geological profile of the BM-7c borehole with sampling places (according to Pavlović, 2014); b) Cumulative distribution of average content of major and minor elements from the BM-7c borehole; and c) Linear distribution of average content of major and minor elements from the BM-7c borehole.

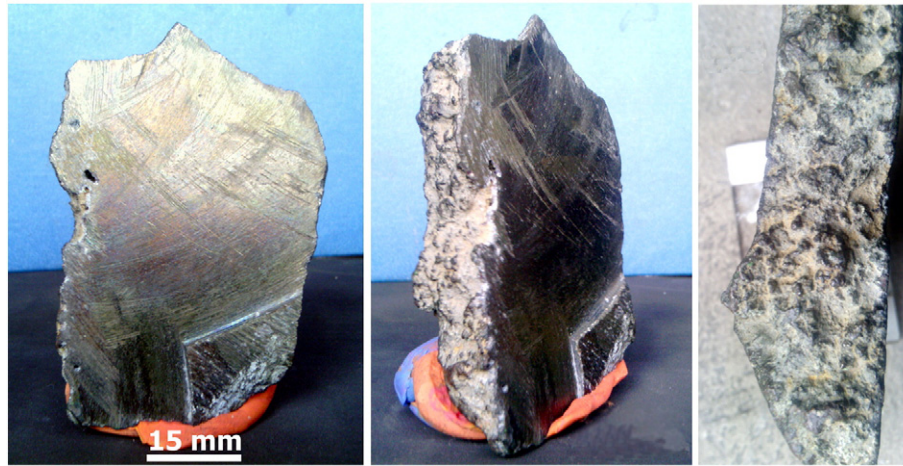


Fig. 4. Macroscopic look of a (Ni-Sb)-bearing Cu-arsenide aggregate from the Mlakva deposit (from different angles).

diffractometer with a Cu tube operated at 40 kV and 30 mA. The instrument was equipped with a diffracted beam curved graphite monochromator and a Xe-filled proportional counter. The diffraction data were collected in the 2θ Bragg angle range from 5 to 70°, counting for 0.50 s (qualitative identification) and from 20 to 80° for 8 s (Rietveld refinement) at every 0.02° step. The divergence and receiving slits were fixed to 1 and 0.1, respectively. All the XRD measurements were performed at room temperature in a stationary sample holder. The unit-cell parameters of β -domeykite, Ni-bearing koutekite, nickeline, native lead, litharge, chalcocite, as well as occupancies of mixed Cu/Ni sites of β -domeykite and Ni-bearing koutekite were obtained by the full structure matching mode of the Rietveld method (Rietveld, 1969) using the MAUD software (Lutterotti, 2009).

4. Bulk ore geochemistry

Copper, Fe, Bi and Ag, locally As, Ni, Mo and W are the most economically important metals at Mlakva deposit. According to the chemical analyses of the borehole BM-7c (Fig. 2, profile AA'), the composition of the ore shows variable content of metallic elements (Table 1). The Pb and Zn contents are extremely low, 0.01 and 0.02 wt%, respectively.

The content of Fe is very variable and ranges from 4.63 to 41.90 wt.% (average 27.71 wt.%; CV = 56%); CV (coefficient of variation) = (standard deviation / mean) \times 100. The Cu content in the ore composite ranges from 0.34 to 2.43 wt.% (average 0.88 wt.%; CV = 75%). The silver content ranges from 3 to 39 g/t (average 10 g/t; CV = 112%). The bismuth content ranges from 0.009 to 0.169 wt.% (average 0.056 wt.%, CV = 89%). The average content of W amounts to 0.006 wt.%. The maximum content of Au is up to 0.2 g/t, and is almost completely absent in the ore deposits of the BOF, although it has been found in the Veliki Cip skarn-replacement Pb-Zn deposit (Fig. 1; Radosavljević et al., 2008).

Contents of minor- and trace-elements are as follows (minimum and maximum, in g/t): Be 0.3–1; Cd 0.3–6.1; Ce 1.3–19; Cr 1–337; Cs 1.2–58.8; Ga 2.3–17.1; Ge 0.1–2.6; Hf <0.1–0.2; Hg <0.1–0.1; In 0.4–13.4; La 0.7–9.4; Li 0.4–20.1; Mn 170–1500; Nb 0.1–1.1; P 100–1100; Sc 0.3–4.8; Se 0.3–4.8; Te 0.8–65.4; Ti 500– > 1000; U 0.8–4; V 5–33; Y 1.2–6; Zr 0.5–7.

Cumulative and linear distributions of average contents of main ore and trace elements in the BM-7c borehole (Fig. 2b) are shown in Fig. 3b–c. According to this, Cu, Ag, Bi, Co and Ni are concentrated (>80%) within the massive and stockwork/disseminated ore, while the W, Sn, and Mo are the most abundant (>70%) elements in altered skarns and dacite-andesites. Other elements are scattered within all defined geological

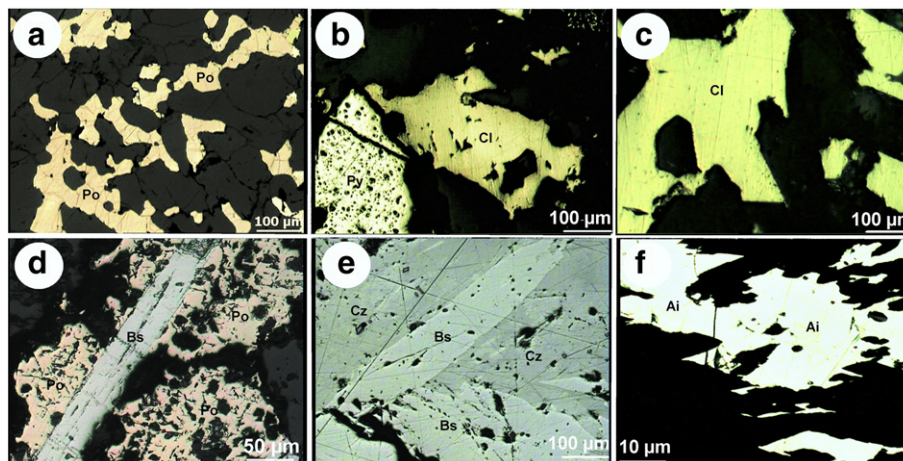


Fig. 5. Reflected light photomicrographs of the pyrrhotite-chalcopyrite-pyrite and Pb(\pm Cu)-Bi sulfosalts mineral assemblage of the Mlakva deposit: a) an anhedronal pyrrhotite aggregate embedded into interspaces of silicate matrix (black) (reflected light, air, //N); b) cataclased pyrite aggregates accompanied by chalcopyrite and silicate gangue minerals (reflected light, air, //N); c) a coarse crystalline chalcopyrite aggregate deposited into interspaces of silicate matrix (reflected light, air, //N); d) an elongated tabular bursaites crystal intersects a pyrrhotite aggregate (reflected light, air, //N); e) bursaites and cannizzarites as exsolution decomposition products in a bursaites aggregate (reflected light, air, //N); f) aikinite embedded into interspaces of silicate matrix (reflected light, oil, //N); Mineral abbreviations: Po – pyrrhotite, Cl – chalcopyrite, Py – pyrite, Bs – bursaites, Cz – cannizzarite, Ai – aikinite.

areas. A correlation analysis was carried out in order to obtain a ratio between main ore and micro-elements within the Mlakva deposit. According to the Pearson coefficient, the best positive correlation was determined between the Cu and Ag ($r = 0.958$).

5. Ore mineralogy

The ore composition in the Mlakva deposit is as follows: sulfides (pyrrhotite, pyrite, marcasite, chalcopyrite, cubanite, mackinawite, valleriite, covelline, chalcocite, arsenopyrite, bismuthinite, molybdenite, sphalerite, and galena), arsenides and antimonides (β -domeykite, Ni-bearing koutekite, (Ni-Sb)-bearing α -domeykite, arsenical breithauptite, nickeline), sulfosalts (bursaitite, cannizzarite, aikinite), native metals (bismuth, silver, lead), oxides (magnetite, hematite, rutile, anatase, and litharge), tungstates and

molybdates (scheelite, powellite), and gangue minerals (quartz, silicates, calcite, apatite, malachite, azurite, Cu-limonite). The main ore minerals are briefly described by their genetic status and paragenetic relations in the mineralization cycle.

5.1. Pyrrhotite-chalcopyrite-pyrite and Pb(\pm Cu)-Bi sulfosalts mineral assemblage

Pyrrhotite occurs in various amounts (from 10 to 90 wt%) as tabular and elongated aggregates (Fig. 5a). The final transformation of pyrrhotite through secondary changes in marcasite and pyrite resulted in typical “bird’s eye” structure. EPMA shows that pyrrhotite has up to 0.04 wt% Co, up to 0.18 wt% Ni, and up to 0.2 wt% Cu (Radosavljević, 1988).

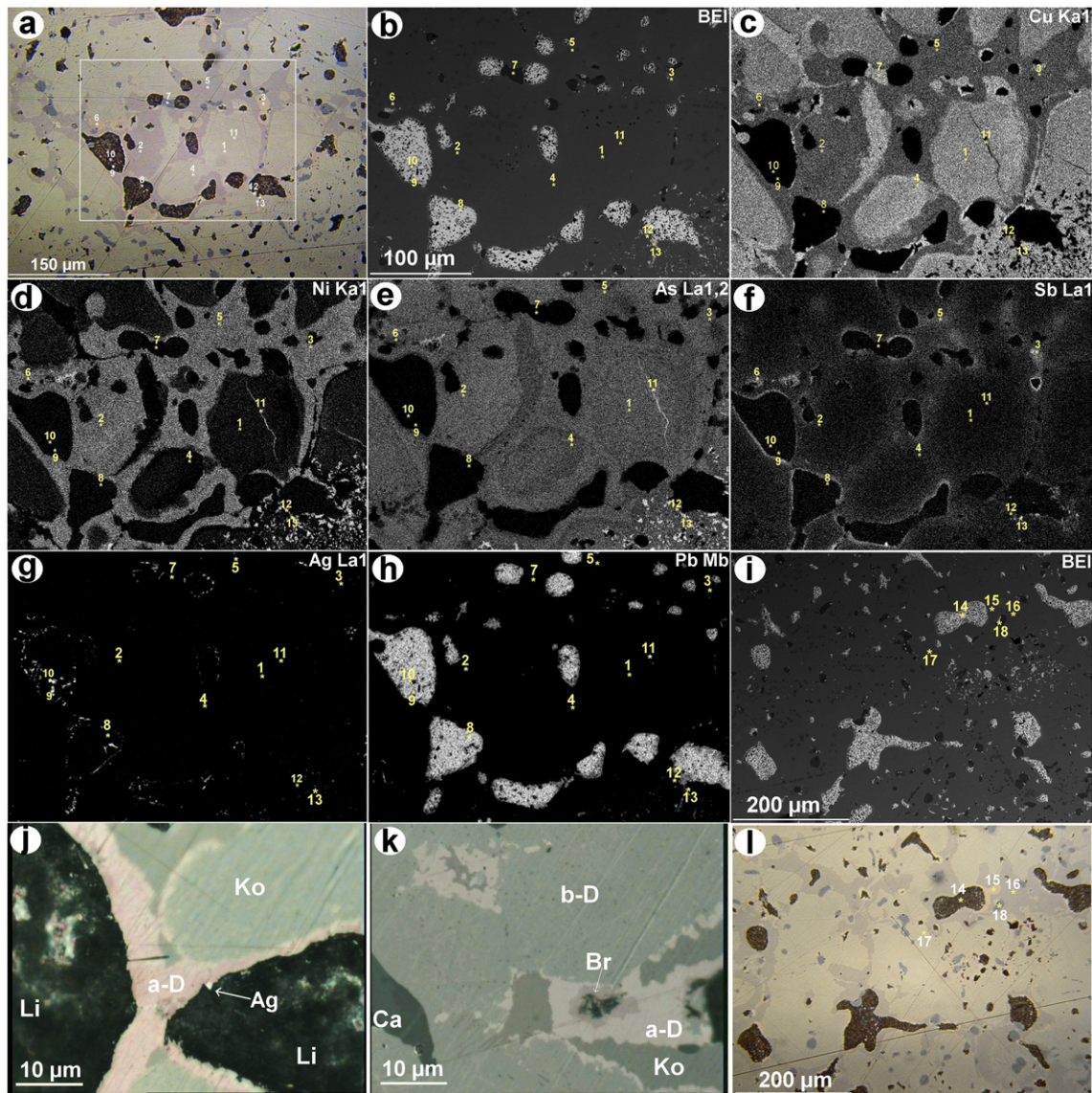


Fig. 6. Reflected light and SEM photomicrographs with an X-ray elemental mapping of Cu-Ni-Sb-bearing arsenides, native Ag and Pb, and chalcocite of the Mlakva deposit: a) β -domeykite (light pink) surrounded by Ni-bearing koutekite (violet greyish), native Pb (black), chalcocite (dark bluish grey), α -domeykite (intensive pink) (numbers 1–13 mark analytical spots; reflected light, air, //N); b) the framed motif from Fig. 6a, with analytical spots (SEM-BEI); c–h) an X-ray elemental mapping from the Fig. 6a–b; i) a SEM image of the Fig. 6l motif (Tables 2 and 3, numbers 14–18 mark analytical spots, SEM-BEI); j) α -domeykite rim (intensive pink) around Ni-bearing koutekite (violet greyish) and native Pb (black) with a droplet of native Ag (reflected light, oil, //N); k) substitution of As-bearing breithauptite (dark pink) with α -domeykite (light pink) accompanied with chalcocite (dark grey) in koutekite matrix (violet grey), (reflected light, oil, //N); l) β -domeykite (light pink) surrounded by Ni-bearing koutekite (violet greyish), native Pb (black), chalcocite (dark bluish grey), α -domeykite (intensive pink) (numbers 14–18 mark analytical spots; reflected light, air, //N); Mineral abbreviations: b-D – β -domeykite (1, 4, 12, 17), a-D – α -domeykite (3, 5, 6, 15), Ko – Ni-bearing koutekite (2, 16); Br – arsenical breithauptite (13), Ni – nickeline (11), Ca – chalcocite (7, 18), Ag – native silver (9, 10), Pb – native lead (8), Li – litharge (14).

Pyrite is the dominant sulfide mineral in the deposit. It is mostly a product of hydrothermal transformation of pyrrhotite. Minor pyrite was deposited directly from hydrothermal solutions when associated with younger chalcopyrite and sulfosalts (Fig. 5b). It is usually overgrown by idiomorphic arsenopyrite crystals. EPMA show that pyrite contains up to 0.03 wt% Co, up to 0.01 wt% Ni, up to 1.5 wt% As and up to 0.07 wt% Cu (Radosavljević, 1988).

Chalcopyrite represents the principal ore mineral in the deposit (Fig. 5c). It is associated with pyrrhotite, pyrite, magnetite, and Pb(Cu)-Bi sulfosalts, and occurs as coarse-grained aggregates, or replaces earlier silicates, oxides, and sulfides. It contains numerous sphalerite and Cu-bearing pyrrhotite star-shaped intergrowths. Cubanite, mackinawite, covelline and valleriite fill cracks and fissures in chalcopyrite aggregates. Arsenopyrite, molybdenite, sphalerite and galena are rare.

Sulfosalts associated with the pyrrhotite-chalcopyrite-pyrite mineral assemblage are represented by lillianite homologue (bursaite), cannizzarite and aikinite. Bi-sulfosalt aggregates were embedded in a garnet-pyroxene matrix. Bursaite forms complex intergrowths with other sulfosalts, and fills cracks and fissures between pyrrhotite, chalcopyrite and silicates (Fig. 5d). Locally, it occurs in lath-like grains, triangular sections and polysynthetic lamellae. In comparison with other accompanying Pb-Bi sulfosalts, it is harder, and often contains inclusions of native bismuth as an exsolution decomposition product. Optically, it is identical to bursaite from the Kram and Kolarica deposits (Radosavljević-Mihajlović et al., 2007). Cannizzarite reflectance is moderately high, but lower than bursaite (Fig. 5e). Bireflectance is distinct, light grey to creamy, anisotropy is strong, similar to bursaite, and hardness is considerably lower (similar to galena). Aikinite is the least abundant sulfosalt. It occurs in the form of elongated crystals, located in the silicate interstices in association with chalcopyrite (Fig. 5f). Hardness is the highest of all sulfosalts of this group. Bireflectance is distinct in air, (strong in oil), light yellow to grey. Anisotropy is also distinct in air (rather high in oil).

5.2. (Ni-Sb)-bearing Cu-arsenides mineral assemblage with native Ag and Pb

The (Ni-Sb)-bearing Cu-arsenides mineral assemblage with native Ag and Pb appears in a form of spherical masses, precipitated in the fissures and hollows of the massive sulfide ore, overall size the space up to

16 cm. (Figs. 3b and 4). It is isolated with thin layer a milky-white clay-carbonates powder from massive sulfide ore. These mineral assemblages were determined only in the BM-7c borehole, and this is the first occurrence within the BOF, PMD, and SMMP.

The (Ni-Sb)-bearing Cu-arsenides occur in aggregates with botryoidal and massive texture composed of rounded grains (Fig. 4). Generally, well-developed crystals are extremely rare (Uytenbogaardt and Burke, 1985). The color of the fresh fracture of the ore is tin white to pale yellowish. These minerals easily oxidize to give the effect of tarnish (brown) and finally iridescence. The streak is steel grey with metallic luster. They are a good conductor of heat and electricity, but not magnetic (700 gauss). Measured specific density of (Ni-Sb)-bearing Cu-arsenide aggregate amounts to $8.06 \pm 0.02 \text{ g/cm}^3$.

XRF chemical analysis powder sample and quantitative EDX analysis of defined areas on polish section of (Ni-Sb)-bearing Cu-arsenides (Fig. 6i), are presented in Table 2. According to these analyses they are practically identical confirming the homogeneous chemical composition of the principal elements (Cu, As, Ni, Pb, Sb and Fe) in the micro (~0.1 mg) and macro (10 g) samples of (Ni-Sb)-bearing Cu-arsenides, which is conditioned by very intimate intergrowths of these minerals. In addition, there is a noticeable content of Ag = 0.19, Bi = 0.11, and Sn = 0.13 wt% and other elements (Table 2).

The (Ni-Sb)-bearing Cu-arsenides occur in rounded and irregular grains of various sizes, accompanied by chalcocite, nickeline, arsenical breithauptite, native silver, native lead, and litharge (Fig. 6a, l). Their reflectance is high, and on the basis of color impression two main mineral phases can be distinguished: β -domeykite and koutekite. When exposed to air these minerals quickly oxidize in blue or purple tinge.

The most abundant mineral among (Ni-Sb)-bearing Cu-arsenides is β -domeykite. It commonly occurs as fine oval to circular grains from 10 to 150 μm (Figs. 6a, l). Color is light creamy with a pink tinge (stronger in oil immersion). It has relatively high reflectance (R=45%). Bireflectance and the effects of anisotropy are commonly covered with iridescence. The atomic proportions of each element were calculated on the basis of empirical formula (Cu_3As). EPMA yielded an average crystallochemical formula: $(\text{Cu}_{2.71}, \text{Ni}_{0.16}, \text{Fe}_{0.03}, \text{Ag}_{0.01}, \text{Pb}_{0.01})_{\Sigma 2.92} (\text{As}_{0.99}, \text{Sb}_{0.06}, \text{S}_{0.02})_{\Sigma 1.07}$ (4 analyses). It is characterized by increased contents of Ni (0.26–6.00 wt%), Sb (2.00–2.60 wt%), Fe (<0.3–1.20 wt%), and Ag (<0.3–1.61 wt%) (Tables 3 and 4).

Koutekite occurs as cement to oval β -domeykite and native lead (Fig. 6c–e). As a rule, β -domeykite is overgrown by koutekite. These

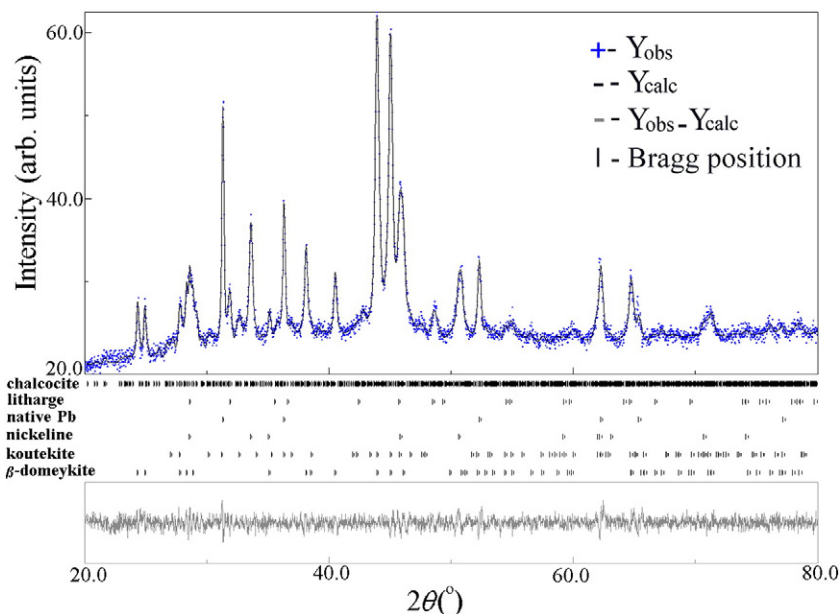


Fig. 7. Rietveld refinement plot of the concentrate sample of (Ni-Sb)-bearing Cu-arsenides from the Mlakva deposit.

Table 2
Chemical analyses of the (Ni-Sb)-bearing Cu-arsenide aggregate obtained by different chemical methods (in wt%).

	O	Cu	As	Sb	Ni	Co	Ag	Bi	Fe	Mn	Cd	Te	Sn	Pb
1	n.a.	49.00	27.95	2.70	7.10	0.05	0.19	0.11	1.15	0.04	0.01	0.08	0.13	9.88
2	1.8	50.9	26.9	2.8	7.0	n.d.	n.d.	n.d.	1.0	n.d.	n.d.	n.d.	n.d.	9.8

Note: n.a. not analyzed; n.d. not detected (<0.3 wt%); 1. – XRF analyses (Se < 0.009 wt%, Au and Zn not detected); 2. – Quantitative EDX analyses (SA = $0.4 \times 0.6 = 0.24 \text{ mm}^2$; V = $0.24 \times 0.03 = 0.0072 \text{ mm}^3$; W = $0.0072 \text{ mm}^3 \times 8.06 \text{ mg/mm}^3 = 0.058 \text{ mg}$).

intimate intergrowths of two minerals make an impression of a micro pseudo-brecciated structure. Among (Ni-Sb)-bearing Cu-arsenides, koutekite has the lowest reflectance; violet-grey color with a bluish tinge. Bireflectance and anisotropy are not visible. The atomic proportions of each element were calculated on the basis of empirical formula (Cu_5As_2). EPMA gave an average crystallochemical formula: $(\text{Cu}_{3.40}, \text{Ni}_{1.40}, \text{Fe}_{0.11})_{\Sigma 4.91} (\text{As}_{1.94}, \text{Sb}_{0.13}, \text{S}_{0.02})_{\Sigma 2.09}$ (2 analyses). Koutekite is characterized by the high contents of Ni (17.40 to 17.61 wt%) and increased contents of Sb (2.90–4.00 wt%), and Fe (1.20–1.50 wt%) (Tables 3 and 4).

α -domeykite, occurs in a form of rims around koutekite or in contacts with native silver and lead (Fig. 6j). Compared to all present (Ni-Sb)-bearing Cu-arsenides it has the highest reflectance; intensive pink-orange color. Bireflectance and anisotropy are not visible. The atomic proportions of each element were calculated on the basis of empirical formula (Cu_3As). EPMA gave an average crystallochemical formula: $\text{Cu}_{1.97} (\text{Ni}_{0.98}, \text{Fe}_{0.03})_{\Sigma 1.01} (\text{As}_{0.81}, \text{Sb}_{0.22})_{\Sigma 1.03}$ (4 analyses). It is characterized by the high contents of Ni (20.11 to 21.73 wt%) and Sb (8.40–10.30 wt%) (Tables 3 and 4).

Breithauptite is rare and occurs in small grains (up to 10 μm) (Fig. 6k). Its reflectance is close to Cu-arsenides with strong bireflectance of bright orange to pale pinkish color effects (Fig. 6k). EPMA gave an average crystallochemical formula: $(\text{Ni}_{0.83}, \text{Cu}_{0.18}, \text{Fe}_{0.01}, \text{Pb}_{0.02})_{\Sigma 1.04} (\text{Sb}_{0.61}, \text{As}_{0.35})_{\Sigma 0.96}$ (one analysis). Due to relatively high contents of As, it is described as arsenical breithauptite (Table 3). It is possible that small portions of Cu and As in arsenical breithauptite were resorbed from Ni-bearing koutekite.

Nickeline, the youngest of all arsenides, commonly occurs along fissures and cracks in β -domeykite aggregates or concentrates in contacts of native lead and (Ni-Sb)-bearing Cu-arsenides (Fig. 6c–e). Its reflectance is slightly higher than Cu-arsenides, with noticeable bireflectance of yellow-pink to pale brownish pink color effects (Fig. 6k). EPMA gave an average crystallochemical formula: $(\text{Ni}_{0.66}, \text{Cu}_{0.22}, \text{Fe}_{0.15})_{\Sigma 1.03} (\text{As}_{0.93}, \text{Sb}_{0.03}, \text{S}_{0.01})_{\Sigma 0.97}$ (one analysis). Due to the increasing content of Cu, Fe and Sb (Table 3), this nickeline differs from genetically similar occurrence in South-Western Serbia, Rogozna ore field (Radosavljević et al., 2015).

Native lead is commonly coated with its oxides (dark zones, Fig. 6a, j, and l). Native silver is either embedded in it, or in a form of rims surrounding native lead grains (Fig. 6g). Native lead always occurs in the form of spindles, droplets and blebs (Fig. 6a–f). EPMA gave an average crystallochemical formula: $(\text{Pb}_{0.95}, \text{Cu}_{0.01}, \text{O}_{0.03})_{\Sigma 0.99}$ (one analysis) (Table 3). Similarly to the Mlakva deposits, it was also found in Australia, USA, Argentina, Austria, Poland (Anthony et al., 1990; Carr et al., 2008; etc.).

Native silver generally occurs as fine intergrowths in boundaries of native lead oval grains or near the contact of native lead and Cu-arsenides (Fig. 6j). EPMA gave an average crystallochemical formula: $(\text{Ag}_{0.89}, \text{Pb}_{0.07}, \text{Ni}_{0.02}, \text{Sb}_{0.02})_{\Sigma 1.00}$ (two analysis) (Table 3).

The only sulfide in this mineral assemblage is chalcocite. It usually occurs in elongated or irregular droplets, with characteristic polysynthetic lamellae and strong bireflectance (Fig. 6k). According to EPMA an average crystallochemical formula is as follows: $(\text{Cu}_{1.88}, \text{Fe}_{0.06}, \text{Pb}_{0.01}, \text{Ni}_{0.01})_{\Sigma 1.96} \text{S}_{1.04}$ (two analyses) (Table 3).

5.3. Genetic features of the Mlakva Cu deposit and the Cu-As-Ni-Sb-Pb mineralization

Mlakva can be classified as a Ca-type skarn-replacement hydrothermal deposit. It consists of large masses of calcite-garnet-pyroxene and pyroxene-amphibole rocks with magnetite, scheelite and powellite. The high-temperature hydrothermal stage is divided in several sub-stages. Deposition order of minerals in the Mlakva Cu deposit is reported in Table 5. The high-temperature hydrothermal pyrrhotite-chalcocopyrite-pyrite and $\text{Pb}(\pm \text{Cu})\text{-Bi}$ sulfosalts mineral assemblage is composed of minerals of low-sulfidation state (pyrrhotite, Fe-rich

Table 3Representative EPMA of β -domeykite, Ni-bearing koutekite, Ni-Sb-bearing α -domeykite, chalcocite, native Ag, native Pb, and litharge from Fig. 6a and l (in wt%).

N ^o	O	S	Fe	Ni	Cu	As	Ag	Sb	Pb	Total	Minerals
1	–	0.30	1.00	3.97	63.90	27.67	–	2.60	–	99.44	β -domeykite
4	–	0.30	0.60	4.03	64.57	27.88	–	2.60	–	99.98	β -domeykite
12	–	–	–	0.26	64.04	28.02	1.61	2.36	3.30	99.59	β -domeykite
17	–	0.30	1.20	6.00	63.75	27.00	–	2.00	–	100.25	β -domeykite
3	–	–	0.58	21.07	46.08	22.24	–	9.78	–	99.73	α -domeykite
5	–	–	0.50	21.27	44.29	23.70	–	10.30	–	100.16	α -domeykite
6	–	–	0.70	21.73	45.45	21.72	–	10.30	–	99.90	α -domeykite
15	–	–	0.70	20.11	47.27	23.42	–	8.40	–	99.90	α -domeykite
7	–	21.19	2.54	0.64	73.59	–	–	–	1.84	99.80	Chalcocite
18	–	21.00	1.30	0.40	77.50	–	–	–	–	100.20	Chalcocite
9	–	–	–	0.91	–	–	84.54	3.19	10.86	99.50	Native Ag
10	–	–	–	1.01	0.35	–	82.54	1.77	13.44	99.11	Native Ag
2	–	0.30	1.50	17.40	46.35	31.47	–	2.90	–	99.92	Ni-bearing koutekite
16	–	–	1.20	17.61	45.91	30.81	–	4.00	–	99.53	Ni-bearing koutekite
8	0.40	–	–	–	1.10	–	–	–	98.80	100.30	Native Pb
11	–	0.21	6.14	28.58	10.09	51.57	–	3.01	–	99.60	Nickeline
14	6.20	–	–	–	0.50	–	–	–	93.40	100.10	Litharge
13	–	–	0.17	29.17	7.03	15.63	–	44.62	2.68	99.30	Arsenical breithauptite

Note: N^o number of analysis (analytical spot in Fig. 6a and l); – not detected (<0.3 wt%); Bi and Co contents <0.3 wt%.

sphalerite) deposited from low alkaline fluids (e.g. presence of pyrrhotite, Fe-rich sphalerite; according to Einaudi et al., 2003). The change of pH and Eh conditions, as well as the sulfidization of pre-existing sulfides led to hydrothermal paragenetic sequence of pyrrhotite → marcasite → pyrite (Ramdohr, 1980). Change of pH and temperature when the depositional environment become more alkaline led to deposition of sulfosalts with Bi, Pb and \pm Cu (bursaite, cannizzarite, aikinite, Mozgova et al., 1987; Radosavljević-Mihajlović et al., 2007).

The main ore metals of the Mlakva deposit, derived from a common magmatic source, which is considered to be granodiorite of Boranja, are Cu, Fe, Bi and Ag, and locally As, Ni, Mo and W (Table 1; Rakić, 1962). According to δS^{34} isotopic analyses of stibnite from the Rujevac Sb-Pb-Zn-As deposit (Fig. 1), ranging from +0.03 to –1.97‰, average –0.54‰, sulfur from sulfides, sulfarsenides, and sulfosalts is of magmatic origin (Mudrinić, 1984). Minor fluctuations of δS^{34} are a function of crystallization temperatures. If low-temperature hydrothermal ore-fluids had a magmatic origin, it can be assumed that the high-temperature ore-fluids had a common origin. This was previously confirmed by a

paragenetic analysis of Pb-Zn mineral associations within SMMP (Rakić, 1962). Temperatures of deposition of Pb-Zn mineral associations in the BOF range from 480 to 160 °C. Galena and sphalerite genesis spans all high- to low-temperature hydrothermal stages, while the Pb-Zn mineral associations of the Veliki Cip and Ravna deposits correspond to the high- (480 °C) and low-temperature hydrothermal stages (230 °C), respectively. In addition, the Veliki Majdan ore zone corresponds to a temperature range from 450 to 367 °C that is between high- and medium-temperature hydrothermal stages (Radosavljević et al., 2012). Temperatures of ore formation gradually decrease moving further away from the Boranja granodiorite according to the following sequence: Mlakva → Kram → Kolarica → Centralni revir → Kojići (Fig. 1).

The mineralization of (Ni-Sb)-bearing Cu-arsenides with Pb and Ag was precipitated in the fissures and hollows of the massive sulfide ore. It was determined only in samples from the BM-7c borehole (Fig. 2, profile AA'). Its presence is unexpected, and its genesis unclear, however, ore relationships at Mlakva suggest the following processes may have played a role in their formation:

Table 4Representative average EPMA and atomic proportions of β -domeykite, α -domeykite and koutekite from different deposits (in wt%).

Locality	(n)	Mineral	S	Fe	Ni	Cu	As	Ag	Sb	Pb	Total
Mlakva, Serbia ¹	4	β -domeykite	0.30	0.70	3.57	64.07	27.64	0.40	2.93	0.83	99.82
Černý Důl, Czech Republic ²	6	β -domeykite	n.d.	0.17	n.d.	70.09	29.39	0.03	n.d.	n.a.	99.68
Mlakva, Serbia ¹	4	α -domeykite*	n.d.	0.58	21.07	46.08	22.24	n.d.	9.78	n.d.	99.73
Mohawk, USA ³	2	α -domeykite	n.a.	n.a.	n.d.	71.00	28.60	n.a.	n.a.	n.a.	99.60
Wasserfall, France ⁴	?	α -domeykite	0.06	n.a.	n.a.	71.16	28.27	n.a.	0.12	n.a.	99.61
Mlakva, Serbia ¹	2	Ni-bearing koutekite	0.15	1.35	17.51	46.13	31.14	n.d.	3.45	n.d.	99.73
Černý Důl, Czech Republic ²	5	koutekite	n.d.	0.05	n.d.	67.05	33.22	0.03	n.d.	n.a.	100.36
Daluis, France ⁴	?	koutekite	n.a.	n.d.	n.a.	68.20	32.50	n.a.	n.a.	n.a.	100.70
Wasserfall, France ⁴	?	koutekite	n.a.	0.10	n.a.	67.98	31.60	n.a.	n.a.	n.a.	99.77
Kazakhstan ⁵	2	koutekite	n.a.	n.a.	n.a.	66.79	33.44	n.a.	n.a.	n.a.	100.23
apfu											A/B
Mlakva, Serbia ¹		β -domeykite	0.02	0.03	0.16	2.71	0.99	0.01	0.06	4	2.73
Černý Důl, Czech Republic ²		β -domeykite		0.01		2.96	1.05			4	2.74
Mlakva, Serbia ¹		α -domeykite*		0.03	0.98	1.97	0.81		0.22	4	2.83
Mohawk, USA ³		α -domeykite				2.98	1.02			4	2.92
Wasserfall, France ⁴		α -domeykite				2.99	1.01			4	2.96
Mlakva, Serbia ¹		Ni-bearing koutekite	0.02	0.11	1.40	3.40	1.94		0.13	7	2.35
Černý Důl, Czech Republic ²		koutekite				4.93	2.07			7	2.38
Daluis, France ⁴		koutekite				4.98	2.01			7	2.48
Wasserfall, France ⁴		koutekite		0.01		5.01	1.98			7	2.53
Kazakhstan ⁵		koutekite				4.91	2.09			7	2.35

Note: n.d. not detected; n.a. not analyzed; (n) number of analysis; apfu atoms per formula unit; * - Ni-Sb-bearing α -domeykite; A = Σ Cu + Fe + Ni + Ag; B = Σ As + Sb + S; A/B atomic ratio; ¹this study; ²Johan, 1985; ³Moore, 1971; ⁴Anthony et al., 1990; ⁵Abulgazina et al., 1991.

Table 5

Deposition order of ore and gangue minerals within the Mlakva deposit (according to Radosavljević, 1988, updated by this study).

Stages	Minerals
Pyrometamorphic (skarn)	Calcite I – garnet (andradite) – pyroxenes – epidote – chlorite Magnetite I – scheelite – powellite – rutile – anatase – pyrite I – quartz I
High-temperature hydrothermal	Pyrrhotite I – cubanite – chalcopyrite I – sphalerite I – Cu-bearing pyrrhotite – aikinite – bismuthinite – quartz II Calcite II – bursaitite – cannizzarite – native bismuth – magnetite II Arsenopyrite – sphalerite II – galena – molybdenite – quartz III
Transformation (hypogene)	Marcasite – pyrite II – hematite
Thermal melting (?) or high-temperature hydrothermal	β -domeykite – Ni-bearing koutekite – chalcocite – native Pb – native Ag
Low-temperature hydrothermal	(Ni-Sb)-bearing α -domeykite (?) – arsenical breithauptite – nickeline
Supergene	Mackinawite – valleriite – covellite – litharge – malachite – azurite – limonite

- (1) Hydrothermal crystallization of Cu-bearing arsenides is possible only under highly reduced conditions, where fS^{2-} and fO^{2-} are at minimum value, while Cu and As concentrations in ore-bearing solutions are high (Brookins, 1986). Arsenopyrite from the Mlakva deposit, as the principal As mineral is insignificant, but it tends to form small isolated monomineral pockets. Based on literature data (Vink, 1996), arsenopyrite is stable in an alkaline environment under strong reducing conditions. With increased acidity, however, it becomes unstable, producing metallic arsenic (As^0) and Fe^{2+} ions. Precipitation of Cu-bearing arsenides begins with influx of hydrothermal solutions enriched in Cu.
- (2) The great impact on precipitation of Cu-bearing arsenides had relic organic matter widespread in sediments of DCF (Radosavljević et al., 2013). Similarly, arsenic from Saulpe (Austria) was transported as oxidic As^{3+} complexes and was reduced to As^0 in the breccias, where reducing conditions are also indicated by the widespread occurrence of graphite (Göd and Zemann, 2000). In the study published by Johan (1985) the author comes to the same conclusions for the Černý Důl deposit (the Czech Republic). According to Johan (1985), hydrothermal deposition of Cu-bearing arsenides was influenced by organic matter (methane).
- (3) Finally, according to literature data (e.g. Frost et al., 2002; Tomkins et al., 2004, 2006; Biagioni et al., 2013), Cu-bearing arsenides could be remobilized and concentrated into discrete pockets in massive sulfide deposits that have undergone metamorphism. Theoretically, a polymetallic melt may form at temperatures as low as 300 °C, where orpiment and realgar melt. However, for many ore deposits, the first melting reaction would be at 500 °C, where arsenopyrite and pyrite react to

form pyrrhotite and an As–S melt. The melt forming between 500 and 600 °C, depending on pressure, will be enriched in Ag, As, Au, Bi, Hg, Sb, Se, Sn, Tl, and Te, which Frost et al. (2002) term low-melting point chalcophile metals. Contact metamorphism occurred in the Mlakva and Kram mining sectors (Karamata, 1955), so that a polymetallic melt is likely in some parts of the deposit. In addition, thermal effects can be achieved through local post-mineralization tectonic-fault movements, thus surrounding the Mlakva deposit during geological history (Fig. 2b–c). The polymetallic melt and formation of massive mineralization of Cu-bearing arsenides can be defined by the following processes (Habashi, 1984): i) direct melt reduction (reduction of Cu arsenate by CH_4 , CO, H, etc., will yield Cu-As alloys); ii) co-melting (secondary oxy-carbonates Cu minerals are melted together with sulfidic ores of arsenic); iii) cementation (a mixture of arsenic minerals such as $CuFeS_2$, $FeAsS$ or As_2S_3 with organic matter), during which the formation of Cu-As alloys is the most abundant.

6. Crystallographic investigations

XRD analysis of the concentrate sample of (Ni-Sb)-bearing Cu-arsenides from the Mlakva deposit was examined using the Rietveld method. Mineralogical composition of the analyzed sample is as follows: β -domeykite, koutekite, nickeline, native lead, litharge and chalcocite (α -domeykite and arsenical breithauptite were below detection limits). The unit–cell parameters of the main minerals from the Mlakva deposit are shown in Table 6. Mixed Cu/Ni crystallographic sites and occupancies of β -domeykite and koutekite were refined starting from the atomic coordinates published by Mansmann (1965) and Liebisch and Schubert (1971), respectively, in order to obtain whether Ni substituted Cu in some degree in these crystal structures. The full structure matching mode of the Rietveld refinement yielded following agreement factors: $R_w = 4.78$, $R_b = 3.71$, $R_{exp} = 3.78\%$. The unit–cell parameters of (Ni-Sb)-bearing Cu-arsenides are in good agreement with the literature data. β -domeykite from this study lies between the data published by Steenberg (1938) and Gukov et al. (1971), however, it has the lowest calculated density. Koutekite, on the other hand, has smaller unit-cell parameters, but higher calculated density in comparison to the literature data (Liebisch and Schubert, 1971). The Rietveld refinement plot and unit–cell parameters of (Ni-Sb)-bearing Cu-arsenides of the from the Mlakva deposit are presented in Fig. 7 and Table 7, respectively. The Rietveld refinement confirmed EPMA that part of Cu was substituted by Ni. According to the occupancies refined, all three Cu crystallographic sites of both minerals contain Ni, with presence of a small number of vacancies in β -domeykite. The crystallochemical formulae of β -domeykite and koutekite calculated from the Rietveld refinement data are as follows: $(Cu_{2.844}, Ni_{0.087}, \square_{0.069})_{\Sigma 3}As$ and $(Cu_{3.863}, Ni_{1.137})_{\Sigma 5}As_2$, respectively. Based on this analysis, Ni amounts to 1.96 and 14.44% in β -domeykite and koutekite, respectively. Refined occupancies of mixed Cu/Ni crystallographic sites of β -domeykite and koutekite from the Mlakva deposit are given in Table 8.

Table 6

Unit–cell parameters of the main minerals from the Mlakva deposit.

Mineral	S.G.	a (Å)	b (Å)	c (Å)	α (°)	β (°)	γ (°)	V (Å ³)
β -domeykite	165	7.1331(4)	7.1331(4)	7.3042(5)	90	90	120	321.86(2)
Koutekite	72	5.922(4)	11.447(9)	5.480(4)	90	90	90	371.48(5)
Nickeline	194	3.6020(6)	3.6020(6)	5.113(2)	90	90	120	57.45(2)
Native Pb	225	4.9408(4)	4.9408(4)	4.9408(4)	90	90	90	120.61(3)
Litharge	129	3.964(2)	3.964(2)	5.043(4)	90	90	90	79.24(2)
Chalcocite	14	15.292(6)	12.073(6)	13.230(6)	90	116.82(4)	90	2179.78(4)

S.G. - space group: 165 - $P\bar{3}c1$; 72 - *Ibam*; 194 - $P6_3/mmc$; 225 - $Fm\bar{3}m$; 129 - $P4/nmm$; 14 - $P2_1/c$.

Table 7
Unit-cell parameters of β -domeykite and koutekite from the Mlakva deposit in comparison with the literature data.

Mineral	<i>a</i> (Å)	<i>b</i> (Å)	<i>c</i> (Å)	ρ_{calc} (g/cm ³)	<i>V</i> (Å ³)	Reference
β -domeykite	7.1331(4)	7.1331(4)	7.3042(5)	8.07	321.86(2)	This study
β -domeykite	7.16	7.16	7.33	8.13	325.43	1
β -domeykite	7.088	7.088	7.232	8.409	314.66	2
β -domeykite	7.143(3)	7.143(3)	7.324(3)	8.176	323.62	3
β -domeykite	7.102(20)	7.102(20)	7.246(20)	8.36	316.51	4
Koutekite	5.922(4)	11.447(9)	5.480(4)	8.26	371.48(5)	This study
Koutekite	5.977(1)	11.577(2)	5.491(1)	8.174	379.95	5

1 – Berry and Thompson, 1962; 2 – Steenberg, 1938; 3 – Mansmann, 1965; 4 – Gukov et al., 1971; 5 – Liebisch and Schubert, 1971.

7. Discussion and conclusions

In comparison with pyrrhotite-chalcocopyrite-pyrite mineral assemblage, the (Ni-Sb)-bearing Cu-arsenides are younger (Table 5). The β -domeykite crystallized first, thus forming massive aggregates with native Pb and chalcocite eutectics (Ramdohr, 1980; Craig, 2001). The stability of β -domeykite lies in a wide interval from 225 to 827 °C (Chvilyova et al., 1988). It is possible that primary Cu-arsenides were deposited in a form of high-temperature cubic koutekite, and then decomposed peritectically to β -domeykite and native As between 360 and 340 °C. If quenched, the high-temperature phase transforms at 315 °C into a low-temperature, orthorhombic modification identical to koutekite (Juza and von Benda, 1968; Liebisch and Schubert, 1971). Native As is stable under 230 °C (Heinrich and Eadington, 1986), and at higher temperatures becomes part of Cu-arsenides, which is the main reason of non-stoichiometric composition of these minerals (Table 4). In addition, some quantities of native As reacted with solutions enriched with Ni²⁺ and Sb³⁺ cations, thus forming arsenical breithauptite and nickeline (Fig. 6d–f). Finally, massive aggregates of (Ni-Sb)-bearing Cu-arsenides in the Mlakva deposit are practically composed of two minerals (~80 wt%) hexagonal β -domeykite and orthorhombic koutekite (Fig. 4).

The origin of Ni and Cu within the Cu(Bi,Ag)-FeS associations of the BOF is most probably from the Vardar ophiolite zone (Dimou and Papastavrou, 1987; Radosavljević et al., 2015). The Mlakva and Kram mining sectors are genetically related to the intrusive complex of Boranja (Fig. 1). In the Karavansalija, there is also a genetic relation with the volcanic-intrusive complex of Rogozna (southwestern Serbia) with the formation of a low grade Cu-Au-(Mo-Pb-Zn) polymetallic skarn mineralization (Budinov et al., 2015; Radosavljević et al., 2015). This mineralization type is uncommon for Neogene igneous complexes formed along the Vardar ophiolite zone and its rim. According to Janković (1995), Cu and Ni in the magma were probably sourced from the serpentinite basement and surroundings, and were mobilized during magma ascent through the metamorphic rocks. However in the Lavrion deposit Greece (e.g. Clemence mine), the gersdorffite-gold-bismuthinite mineral association is interpreted to be

Table 8
Refined occupancies of mixed Cu/Ni crystallographic sites of β -domeykite and koutekite from the Mlakva deposit.

β -domeykite			Koutekite		
Atom	Wyck. position	Occu. (<1)	Atom	Wyck. position	Occu. (<1)
Cu1	12 g	0.9421	Cu1	8j	0.7541
Ni1	12 g	0.0298	Ni1	8j	0.2459
□	12 g	0.0281	–	–	–
Cu2	4d	0.9578	Cu2	8 g	0.8104
Ni2	4d	0.0274	Ni2	8 g	0.1896
□	4d	0.0148	–	–	–
Cu3	2a	0.9646	Cu3	4b	0.7344
Ni3	2a	0.0254	Ni3	4b	0.2656
□	2a	0.0100	–	–	–

□ - vacancies; Wyck. position - Wyckoff position; Occu. - occupancy.

of magmatic origin, related to dykes of both acidic and basic composition (Voudouris et al., 2008). Large sedimentary deposits of Fe with Ni, Co, and Cr of Cretaceous age have been discovered in Serbia (Janković, 1990). During the Neogene magma inflow through the ophiolitic mélangé within the DCF sediments, ore and post-ore low-temperature hydrothermal solutions remobilized Ni from mafic rocks. The Ni content in massive and stockwork/disseminated Cu ore is about 30 times higher compared to the surrounding rocks (Table 1; Fig. 3b–c). Small amounts of Ni originated from massive pyrrhotite, which is largely affected by a hydrothermal transformation into pyrite and marcasite (Ramdohr, 1980). Hydrothermal solutions enriched with Ni (with constant and variable activity of As and Sb) circulated along the cracks, pores and fissures thus changing primary mineral composition.

Orthorhombic koutekite reacted with nickeliferous solutions thus forming Ni-bearing koutekite. Arsenides and antimonides of Ni are the youngest, filling cracks and fissures of (Ni-Sb)-bearing Cu-arsenides (Fig. 6d–e). Native Pb did not react with the Ni-Sb-bearing solutions due to its inertia to these metals (ASM Handbook, 1992). Furthermore, native Pb entirely expelled Ag on grain boundaries or along contacts with Cu-arsenides (Fig. 6g).

A simplified deposition order of minerals within the (Ni-Sb)-bearing Cu-arsenides mineral assemblage with native Ag and Pb is as follows: β -domeykite → chalcocite → native Pb → native Ag → Ni-bearing koutekite → (Ni-Sb)-bearing α -domeykite → arsenical breithauptite → nickeline → litharge (Table 5). In the Černý Důl deposit, Fe- and Ni-bearing arsenides crystallized first (löllingite → nickeline → parammelsbergite → chloanthite), and then Cu-bearing arsenides with Ag (kutinaite → β -domeykite → koutekite → native Ag → native As → novakite → Cu₂As → paxite → chalcocite). According to data published by Johan (1985), the Černý Důl mineralization extends over a large temperature interval, from about 500 to 100°C. Thus, it differs from those Cu occurrences, which are undeniably of high-temperature origin, as for example, Wasserfall in France (Picot and Ruhlmann, 1978). In the Mohawk deposit (Michigan, USA), minerals encountered and described include α -domeykite, β -domeykite, algodonite, As-bearing copper, koutekite, rammelsbergite, parammelsbergite, and nickeline (Moore, 1971). According to the author, Ni plays no significant role in the decomposition and inversion temperatures of the low-temperature Cu-bearing arsenides since essentially no Ni solid solubility in β -domeykite and koutekite at 510 °C was detected. The same author has determined that EPMA on the naturally occurring low-temperature coexisting As and Ni-Cu-As phases did not afford any detectable evidence for the Ni and Cu-bearing arsenides or Cu in the Ni-bearing arsenides. In addition, in the Anarak District (central Iran), Cu-Fe-bearing sulfides and Ni-Co-bearing arsenides with Bi and U precipitated first and later Cu-bearing arsenides (Tarkian et al., 1983).

It should be taken into account that Moore (1971) conducted his experiments on samples consisting of finely grinded Mohawk material, which were heated in a sealed silica tube for seven days at 510 °C, co-called, “dry sintered”. However, this experiment cannot correspond to hydrothermal deposition processes of native metals and compounds. In natural conditions, the most important parameters are solution activity of given elements in ionic or dispersion nm-compounds (Kolobov

et al., 2001), pH and Eh factors, lithological environments of transportation and deposition settings, temperatures and pressures of hydrothermal processes, etc. (Barton and Skinner, 1979; Pirajno, 1992; Vink, 1996; Valyashko, 2008).

The phenomenon called “aging” of mineral associations is an important mineralogical constituent when native metals and alloys form massive aggregates (Mlakva ~30 Ma). (Ni-Sb)-bearing Cu-arsenides have strong metallic and covalent bonds (Smallman and Bishop, 1999). Massive aggregates of metals and their compounds during very long period of time are affected by the diffusion of metals in the solid state phenomenon. Diffusion of atoms in solids is an extremely slow process. It is practically insignificant at room temperature, and becomes noticeable when the temperature approaches the melting point (Bocquet et al., 1996; Mehrer, 2007; Hosford, 2006). To fulfil this requirement interdiffusion is essential that occurs in materials with different atoms. The most important precondition is the mutual melting of the elements (Cu and Ni) or at least partial melting (Sb and Cu), while in the case where there is no melting diffusion is impossible (Pb and Ni) (Bader et al., 1995; Christian, 2002). Diffusion of metals and their compounds occurs: a) through the volume – atoms move through crystals from one to another crystal lattice or interstitial positions; the activation energy is higher, the diffusion rate lower; b) by metal grain boundaries (surfaces) – easier than through the volume, regularity arrangement of the atoms was violated at metal grain boundaries, smaller packing density of atoms and a large concentration of defects, the activation energy is lower, higher diffusion coefficient and mass flow of atoms (Felberbraun et al., 2011). The movement of atoms is not “continuous” but, they move “jumping” from one equilibrium position to another (regular atomic sites), or via interstitial positions. Mechanisms of replacement are: i) direct exchange; ii) cyclic exchange; iii) vacancy mechanism; iv) interstitial mechanism (two ways); v) crowdion mechanism.

The diffusion of metals in the solid state phenomenon may explain entrance of Ni into Cu-arsenides and crystallization of Ni-bearing koutekite (Christian, 2002). The concentration of Ni is the highest on boundaries of Cu-bearing arsenides, decreasing to the central parts of grains (Fig. 6d). Nickel is the most abundant in (Ni-Sb)-bearing α -domeykite, and the least present in β -domeykite (Table 4). However, there are indications that (Ni-Sb)-bearing α -domeykite precipitated from low-temperature fluids enriched with nickel in a near-surface, low-pressure environment.

The A/B atomic ratio of Cu-arsenides ($A = \text{apfu} \sum \text{Cu} + \text{Fe} + \text{Ni} + \text{Ag}$; $B = \text{apfu} \sum \text{As} + \text{Sb} + \text{S}$) is non-stoichiometric (Table 4), and is often lower than that of stoichiometric. This is a common feature in all known deposits of (Ni-Cu)-bearing arsenides (Moore, 1971; Tarkian et al., 1983; Johan, 1985; Anthony et al., 1990; Abulgazina et al., 1991). The ideal ratio in domeykite (both β and α), and koutekite amounts to 3 and 2.5, respectively (Anthony et al., 1990). Excess of As in Cu-arsenides is the highest in β -domeykite, lesser in koutekite, while in α -domeykite is the smallest (Table 4). Copper arsenides of the well-known deposits worldwide contain neither Ni nor Sb (Table 4), due to different genetic origin. These minerals crystallize later with older mineral assemblages containing Ni-bearing arsenides (Moore, 1971; Johan, 1985; Abulgazina et al., 1991). The hydrothermal nickeliferous mineralization at Mlakva occurs in the final mineralization stages replacing earlier skarn ore stages. It was mostly incorporated in older koutekite by the metal diffusion phenomenon in the solid state, and is present throughout the low-temperature hydrothermal stage accompanied with high activity of As, Ni, and Sb. The metallogeny of Ni characterizes all ore fields and metallogenic zones of SMMP, which are associated with complex multi-component systems (Fe, Zn, Cu, Pb, Sb, As, Ag, and S) (Rakić, 1962; Dimou and Papastavrou, 1987; Janković, 1990; Serafimovski et al., 2010; Radosavljević et al., 2015; etc.). Other mineral assemblages with Ni, As and Sb (excluding Cu) are typical for the majority of ore fields and zones within the SMMP. The management of the mines has not been paying enough attention on any other

valuable metal including Ni, but it is believed that plans for the future will be focused on a detailed study of the nickeliferous mineralization.

Finally, Cu- and Ni-arsenides and other natural alloys were the first metalliferous materials that the human race used as a replacement for stone tools in its earliest history of technological beginning (Uhland et al., 2001).

Acknowledgments

The authors of this study owe great appreciation to our colleague Zoran Pavlović (Geosfera Company Ltd., Belgrade) for supplying the samples and geological documentation of the Mlakva deposit, and to the Institute for Mining and Metallurgy (Bor, Serbia) for chemical analyses of geological samples. This paper is a result of a study of the OI-176016 Project (Magmatism and geodynamics of the Balkan Peninsula from Mesozoic to present day: Significance for the formation of metallic and non-metallic mineral deposits), by the Ministry of Education, Science and Technological Development of the Republic of Serbia, which provided financial supported. The authors would like to express their deepest gratitude Professor Dr. Panagiotis Voudouris and Dr. Irina Melekestseva for their valuable comments and suggestions, and to Robert Kellie, consulting geologist, for proofreading the manuscript. The development of this paper has benefited substantially from their comments. We also acknowledge with thanks the editorial handling of our manuscript by Editor-in-Chief Franco Pirajno.

References

- Abulgazina, S.D., Kotelnikov, P.Y., Sal'kov, S.A., Tasov, B.M., Yarenskaya, M.A., Yasnitskaya, G.P., 1991. New data on koutekite. *Zapiski Vsesoyuznogo Mineralogicheskogo Obshchestva* 120 (2), 49–51 (in Russian).
- Anthony, J.W., Bideaux, R.A., Bladh, K.W., Nichols, M.C., 1990. *Handbook of Mineralogy*. Vol. I. Elements, Sulfides, Sulfosalts. Mineral Data Publishing, Tucson, AZ, USA.
- Bader, S., Gust, W., Hieber, H., 1995. Rapid formation of intermetallic compounds interdiffusion in the Cu-Sn and Ni-Sn systems. *Acta Metall. Mater.* 43 (1), 329–337.
- Barton Jr., P.B., Skinner, B.J., 1979. Sulfide mineral stabilities. In: Barnes, L. (Ed.), *Geochemistry of Hydrothermal Ore Deposits* (H. Wiley-Interscience, New York, USA).
- Berry, L.G., Thompson, R.M., 1962. X-ray powder data for ore minerals: the Peacock atlas. *GSA Memoirs* 85, 1–261.
- Biagioni, C., D'Orazio, M., Vezzoni, S., Dini, A., Orlandi, P., 2013. Mobilization of Tl-Hg-As-Sb-(Ag,Cu)-Pb sulfosalts during low-grade metamorphism in the Alpi Apuane (Tuscany, Italy). *Geology* 41 (7), 747–750.
- Bocquet, J.L., Brebec, G., Limoge, Y., 1996. Diffusion in metals and alloys. In: RW, C., Haasen, P. (Eds.), *Physical Metallurgy Vol. I* (North-Holland, Amsterdam).
- Brookins, D.G., 1986. Geochemical behaviour of antimony, arsenic, cadmium and thallium: Eh-pH diagrams for 25 °C, 1 bar pressure. *Chem. Geol.* 54, 271–278.
- Budinov, D.Z., Yonezu, K., Tindell, T., Gabo-Ratio, A.J., Milutinović, S., Boyce, J.A., Koichiro Watanabe, K., 2015. Copper-gold skarn mineralization at the Karavansalija ore zone, Rogozna Mountain, Southwestern Serbia. *Resour. Geol.* 65 (4), 328–344.
- Carr, F.P., Selleck, B., Stot, M., Williamson, P., 2008. Native lead at Broken Hill, New South Wales, Australia. *Can. Mineral.* 46 (1), 73–85.
- Černý, P., Doubek, Z., Veselovský, F., 2003. Nerosty z Bělovsí u Náchoda – Jiráskova lomu. *Minerál* 11 (6), 406–418.
- Christian, J.W., 2002. *The Theory of Transformation in Metals and Alloys*. Part I (Pergamon, Amsterdam).
- Chvilyova, T.N., Bezsmertnaya, M.S., Spiridonov, E.M., Agroskin, A.S., Papayan, G.V., Vinogradova, R.A., Lebedeva, S.I., Zav'yalov, E.N., Filimonova, A.A., Petrov, V.K., Rautian, L.P., Veshnikova, O.L., 1988. *Manual – Determination of the Ore Minerals on Reflected-Light*. NEDRA, Moscow (in Russian).
- Craig, R.J., 2001. Ore-mineral textures and the tales they tell. *Can. Mineral.* 39, 937–956.
- Cvetković, V., Knežević, V., Pécskay, Z., 2000. Tertiary igneous formations of the Dinarides, Vardar zone and adjacent regions: from recognition to petrogenetic implications. In: Karamata, S., Janković, S. (Eds.), *Geology and Metallogeny of the Dinarides and the Vardar Zone*, Banja Luka-Sarajevo. B&H, pp. 245–253.
- Cvetković, V., Prelević, D., Downes, H., Jovanović, M., Vaselli, O., Pécskay, Z., 2004. Origin and geodynamic significance of tertiary post collisional basaltic magmatism in Serbia (Central Balkan Peninsula). *Lithos* 73, 161–186.
- Dana, D.J., 2008. *Manual of Mineralogy*. Merchant Books (Enl New Re edition).
- Delaloye, M., Lovrić, A., Karamata, S., 1989. Age of Tertiary Granitic Rocks of Dinarides and Vardar Zone. 14th Congress CBGA, Sofia, Bulgaria, pp. 1186–1189.
- Dimou, E., Papastavrou, S.E., 1987. The Lachana's listwenites (SerboMacedonian masiff, N. Greece) and their mineralization (Sb-Ni-Co-As). In: Janković, S. (Ed.), *Mineral deposits of the Tethyan Eurasian metallogenic belt between the Alps and Pamirs*. UNESCO/IGCP Project No 169, Department of Mineral Exploration, Faculty of Mining and Geology, University of Belgrade, pp. 91–99.
- Einaudi, M.T., Hedenquist, J.W., Inan, E.E., 2003. Sulfidation state of hydrothermal fluids: the porphyry-epithermal transition and beyond. In: Simmons, S.F., Graham, I.J. (Eds.), *Volcanic, Geothermal Ore-Forming Fluids: Rulers and Witnesses of Processes within the Earth*. Soc Econ Geol Spec Publ Vol. 10, pp. 285–313.

- Felberbraun, M., Ventura, T., Rappaz, M., Dahle, A.K., 2011. Microstructure formation in Sn-Cu-Ni solders alloys. *JOM J. Miner. Met. Mater. Soc.* 63 (10), 52–55.
- Frost, B.R., Mavrogenes, A.J., Tomkins, A., 2002. Partial melting of sulfide ore deposits during medium- and highly-grade metamorphism. *Can. Mineral.* 40 (1), 1–18.
- Göd, R., Zemann, J., 2000. Native arsenic ± realgar mineralization in marbles from Saualpe, Carinthia, Austria. *Mineral. Petrol.* 70, 37–53.
- Gukov, O.Y., Ugai, Y.A., Pshestanchik, V.R., Domashevskaya, E.P., Sen'kina, L.B., 1971. Copper arsenide Cu_3As and the phase diagram $\text{Cu}_3\text{As} - \text{Cu}_3\text{P}$. *Inorg. Mater.* 7 (8), 1192–1194.
- Gupta, K.P., 2000. Phase diagram evaluations: section II an expanded Cu-Ni-Sn system (copper-nickel-tin). *J. Phase Equilib.* 21 (5), 479–484.
- Habashi, F., 1984. Principles of Extractive Metallurgy. Vol. 3. McGraw Hill, New York.
- Hak, J., Johan, Z., Skinner, B.J., 1970. Kutinaite; a new copper-silver arsenide mineral from Černý Důl, Czechoslovakia. *Am. Mineral.* 55, 1083–1087.
- Handbook, A.S.M., 1992. Vol. 3. Alloy phase diagram. ASTM-International, The materials. Information Company, USA.
- Heinrich, C.A., Eadington, P.J., 1986. Thermodynamic predictions of the hydrothermal chemistry of arsenic and their significance for the paragenetic sequence of some cassiterite-arsenopyrite-base metal sulfide deposit. *Econ. Geol.* 81, 511–522.
- Hosford, W., 2006. Materials Science. Cambridge University Press, Cambridge.
- Iglesias, J.E., Nowacki, W., 1977. Refinement of the crystal structure of alpha domeykite, a structure related to the A15 type. *Z. Kristallogr.* 145, 334–345.
- Janković, S., 1990. The Ore Deposits of Serbia: Regional Metallogenic Settings, Environments of Deposition, and Types. Faculty of Mining and Geology, University of Belgrade, Serbia (In Serbian with English summary).
- Janković, S., 1995. The principal metallogenic features of the Kopaonik district. In: Janković, S. (Ed.), *Geology and Metallogeny of the Kopaonik Mountain*. Belgrade, Serbia, pp. 79–102.
- Johan, Z., 1958. Koutekite; a new mineral. *Nature* 181, 1553–1554.
- Johan, Z., 1960. Koutekite — Cu_2As , ein neues mineral. *Chem. Erde-Geochem.* 20, 217–226 (in German).
- Johan, Z., 1961. Paxite- Cu_2As as a New Copper Arsenide Černý Důl in the Giant Mts. (Krkonoše). *Acta Universitatis Carolinae Geologica*, pp. 77–86.
- Johan, Z., 1985. The Černý Důl deposit (Czechoslovakia): an example of Ni-, Fe-, Ag-, Cu-arsenide mineralization with extremely high activity of arsenic; new data on paxite, novakite and kutinaite. *Tschermaks Mineral. Petrogr. Mitt.* 34, 167–182.
- Juza, R., von Benda, K., 1968. Zur Kenntnis des Cu_3As_2 . *Z. Anorg. Allg. Chem.* 357, 238–246 (in German).
- Karamata, S., 1955. Petrological study of magmatic and contact-metamorphic rocks of Boranja. Bulletin of the natural history museum in Belgrade, Series A 6, 1–130 (In Serbian).
- Karamata, S., Krstić, B., 1996. Terrains of Serbia and neighbouring areas. In: Knežević-Djordjević, V., Krstić, B. (Eds.), *Terrains of Serbia*. Faculty of Mining and Geology, University of Belgrade, Serbia, pp. 25–40.
- Karamata, S., Steiger, R., Djordjević, P., Knežević, V., 1990. New data on the origin of granitic rocks from western Serbia. *Bulletin, Académie Serbe des Sciences et des Arts, Classe des Sciences Mathématiques et Naturelles, Sciences Naturelles* 32, 1–9.
- Kolobov, Y.R., Grabovetskaya, G.P., Ivanov, M.B., Zhilyaev, A.P., Valiev, R.Z., 2001. Grain boundary diffusion characteristic of nanostructured nickel. *Scr. Mater.* 44, 873–878.
- Lechtman, H., 1996. Arsenic bronze: dirty copper or chosen alloy? A view from the Americas. *Journal of Field Archaeology* 23 (4), 477–514.
- Liebisch, W., Schubert, K., 1971. Zur Struktur der Mischung Kupfer-Arsen. *J. Less-Common Met.* 23, 231–236 (in German).
- Lutterotti, L., 2009. MAUD Version 2.33. <http://www.ing.unitn.it/~maud/>.
- Makovicky, M., Johan, Z., 1978. Reflectivity and microhardness of synthetic and natural koutekite, kutinaite and beta-domeykite. *Neues Jb. Mineral. Monat.* 421–432.
- Mansmann, M., 1965. Ueber Verbindungen vom anti- LaF_3 -Strukturtyp. *Z. Kristallogr.* 122, 399–406 (in German).
- Mehrer, H., 2007. *Diffusion in Solids*. Springer.
- Monthel, J., Vadala, P., Leistel, J.M., Cottard, F., Ilić, M., Štrumberger, A., Tošović, R., Stepanović, A., 2002. Mineral Deposits and Mining Districts of Serbia: Compilation Map and GIS Databases. BRGM/RC-51448-FR, pp. 1–67.
- Moore, B.P., 1971. Copper-nickel arsenides of the Mohawk No. 2 mine, Mohawk, Keweenaw Co. Michigan. *Am. Mineral.* 56, 1319–1331.
- Mozgova, N.N., Nenacheva, N.S., Borodaev, Y., Svicov, B.A., Ryabeva, G.E., Gamyarin, N.G., 1987. Novye raznovidnost mineralov iz gruppy sulfosolei. Proceedings of the Russian Mineralogical Society. CXVI 5, pp. 614–628 (in Russian).
- Mudričić, Č., 1984. The origin of the ore components and the geochemical characteristics of the antimony deposits of Serbia and Macedonia (Yugoslavia). Proceedings of 6th Quadrennial International Association on the Genesis of Ore Deposits (IAGOD) Symposium, Stuttgart, Germany, pp. 161–167.
- Paar, W.H., Meixner, H., 1979. Neues aus den Kupfererz-Gängen des Flatschacher Bergbau-Reviere bei Knittelfeld, Steiermark. *Karinthin* 81, 148–150 (in German).
- Pavlović, Z., 2014. The Balance Sheet Ore Reserves of the Mlakva mine. Technical Documentation (study) of Geosfera Ltd. company, Belgrade, pp. 1–84 (in Serbian).
- Picot, P., Johan, Z., 1982. Atlas of Ore Minerals. Elsevier, Amsterdam.
- Picot, P., Ruhlmann, F., 1978. Présence d'arséniures de cuivre de haute température dans le granite des Ballons (Vosges méridionales). *Bull. Mineral.* 101, 563–569 (In French with English abstract).
- Picot, P., Vernet, J., 1967. Un nouveau gisement de koutekite: Le dôme du Barrot (Alpes Maritimes). *Bull. Soc. Fr. Minéral. Cristallogr.* 60, 82–89 (in French).
- Pierrot, R., Picot, P., Féraud, J., Vernet, J., 1974. Inventaire Minéralogique de la France, No 4, Alpes Maritimes, BRGM [MinRec 32:312].
- Pirajno, F., 1992. *Hydrothermal Mineral Deposits. Principles and Fundamental Concepts for the Exploration Geologist*. Springer-Verlag, Berlin, Heidelberg.
- Prelević, D., Foley, S.F., Cvetković, V., Romer, R.L., 2004. Origin of minette by mixing of lamproite and dacite magmas in Veliki Majdan, Serbia. *J. Petrol.* 45 (4), 759–792.
- Radosavljević, S., 1988. Nature of silver in Pb-Zn deposits of the Podrinje metallogenic district: Mineralogy and genetic features (Dissertation) University of Belgrade, Serbia (in Serbian with English summary).
- Radosavljević, S., Kašić, V., Stojanović, J., 2008. Mineralogy of gold in polymetallic deposits of Serbia. Proc. of 9th International Congress for Applied Mineralogy. — Precious Metals, International Council for Applied Mineralogy. 8–10, pp. 195–197 (September, Brisbane, Australia).
- Radosavljević, A.S., Stojanović, N.J., Pačevski, M.A., 2012. Hg-bearing sphalerite from the Rujevac polymetallic ore deposit, Podrinje Metallogenic District, Serbia: compositional variations and zoning. *Chem. Erde-Geochem.* 72, 237–244.
- Radosavljević, A.S., Stojanović, N.J., Radosavljević-Mihajlović, S.A., Kašić, D.V., 2013. Polymetallic mineralization of the Boranja ore field, Podrinje Metallogenic District, Serbia: Zonality, mineral associations and genetic features. *Period. Mineral.* 82 (1), 61–87.
- Radosavljević, A.S., Stojanović, N.J., Radosavljević-Mihajlović, S.A., Vuković, S.N., 2014. Rujevac Sb-Pb-Zn-As polymetallic deposit, Boranja ore field, Western Serbia: native arsenic and arsenic mineralization. *Mineral. Petrol.* 108, 111–122.
- Radosavljević, A.S., Stojanović, N.J., Vuković, S.N., Radosavljević-Mihajlović, S.A., Kašić, D.V., 2015. Low-temperature Ni-As-Sb-S mineralization of the Pb(Ag)-Zn deposits within the Rogozna ore field, Serbo-Macedonian Metallogenic Province: ore mineralogy, crystal chemistry and paragenetic relationships. *Ore Geol. Rev.* 65, 213–227.
- Radosavljević-Mihajlović, S.A., Stojanović, N.J., Dimitrijević, Ž.R., Radosavljević, A.S., 2007. Rare Pb-Bi sulfosalt mineralization from the Boranja ore field (Podrinje district, Serbia). *Neues Jb. Mineral. Abh.* 184 (2), 217–224.
- Rakić, S., 1962. Classification of genetic types of Pb-Zn deposits related to Tertiary magmatism in the Dinarides on the basis of characteristics mineral assemblages. Proceedings of the Presentations V Counselling, Geological Association of Companies F.N.R. Yugoslavia, part II Mineralogy-Petrology-Ore Deposits, Belgrade, pp. 189–195 (In Serbian and German).
- Ramdohr, P., 1980. *The Ore Minerals and Their Intergrowths*. Pergamon Press, Oxford.
- Rietveld, H.M., 1969. A profile refinement method for nuclear and magnetic structures. *J. Appl. Crystallogr.* 2, 65–71.
- Sarp, H., Černý, R., 2001. Theoparacelsite, $\text{Cu}_3(\text{OH})_2\text{As}_2\text{O}_7$, a new mineral: its description and crystal structure. *Arch. Sci.* 54, 7–14.
- Serafimovski, T., Stefanova, V., Volkov, A.V., 2010. Dwarf copper-gold porphyry deposits of the Buchim-Damjan-Borov Dol ore district, Republic of Macedonia (FYROM). *Geol. Ore. Deposits* 52, 179–195.
- Smallman, R.E., Bishop, R.J., 1999. *Modern Physical Metallurgy and Materials Engineering*. 6th Edition. Butterworth-Heinemann, Linacre House, Jordan Hill, Oxford.
- Steenberg, B., 1938. The crystal structure of Cu_3As and Cu_3P . *Arkiv för Kemi, Mineralogi och Geologi*, A 12 (2), 1–15.
- Steiger, R.H., Knežević, V., Karamata, S., 1989. Origin of some granitic rocks from the Southern Margin of the Pannonian basin in Western Serbia, Yugoslavia. 5th Meeting of the EUGS, Strasburg, Terra Abstracts 1, 52–53.
- Subramanian, P.R., Launglin, D.E., 1988. The As-Cu (arsenic-copper) system. *Bull. Alloy Phase Diagr.* 9 (5), 605–617.
- Tarkian, M., Bock, W.D., Neuman, M., 1983. Geology and mineralogy of the Cu-Ni-Co-U ore deposits at Talmessi and Meeskani, central Iran. *Tschermaks Mineral. Petrogr. Mitt.* 32 (2–3), 111–133.
- Tomkins, A.G., Pattison, D.R.M., Zaleski, E., 2004. The Hemlo gold deposit, Ontario: an example of melting and mobilization of a precious metal – sulfosalt assemblage during amphibolite facies metamorphism and deformation. *Econ. Geol.* 99, 1063–1084.
- Tomkins, A.G., Frost, R.B., Pattison, D.R.M., 2006. Arsenopyrite melting during metamorphism of sulfide ore deposit. *Can. Mineral.* 44, 1045–1062.
- Uhland, S., Lechtman, H., Kaufman, L., 2001. Assessment of the As-Co-Ni system: an example from archaeology. *Calphad* 25 (1), 109–124.
- Uytenbogaardt, W., Burke, E.A.J., 1985. Tables for Microscopic Identification of Ore Minerals. 2 revised edition. Dover Publications.
- Valyashko, V.M., 2008. *Hydrothermal Properties of Materials: Experimental Data on Aqueous Phase Equilibria and Solution Properties at Elevated Temperatures and Pressures*. A John Wiley & Sons, Ltd., Publication, Printed and bound in Singapore by Markono Print Media Pte Ltd, Singapore.
- Vink, W.B., 1996. Stability of antimony and arsenic compounds in the light of revised and extended Eh-pH diagrams. *Chem. Geol.* 130, 21–30.
- Voudouris, P., Melfos, V., Spry, P.G., Bonsall, T.A., Tarkian, M., Solomos, C., 2008. Carbonate-replacement Pb-Zn-Ag ± Au mineralization in the Kamariza area, Lavrion, Greece: mineralogy and thermochemical conditions of formation. *Mineral. Petrol.* 94, 85–106.